

Replies to Anonymous Referee #1

This paper proposes a new method to estimate the spatial distribution of soil water storage capacity in catchments based on DEM and long-term water balance data. The shape parameter of the distribution is estimated based on HAND values derived from DEM. The average storage capacity over a catchment is estimated, by the MCT method, from climatological and vegetation data (i.e., long-term precipitation, runoff and seasonal NDVI). This method is evaluated in an experimental catchment and MOPEX catchments. This paper provides a novel method to estimate the spatial distribution of soil water storage capacity, which is an important feature for catchment hydrology but is usually not available. I have some comments for the authors to consider before the publication.

Reply: We thank the Anonymous Reviewer #1 for recognising the innovation and the importance of this paper. We also appreciate all his/her constructive comments, which are valuable to improve the quality of this manuscript. For the detailed comments, please find our responses in below.

Comments:

1. As shown in Figure 2, saturated area and runoff coefficient is dependent on the initial soil moisture condition (S_u/S_{uMax}). However, within a time step (daily in this paper), rainfall in the early time causes the increases of S_u/S_{uMax} and runoff coefficient. Therefore, the runoff coefficient during a day is also affected by rainfall, and runoff coefficient is a function of S_u/S_{uMax} , β , and S_{uMax}/P_e (Moore, 1985; Wang, 2018). Given the values of S_u/S_{uMax} and β , equation 12 in Table 2 underestimates R_u/P_e in a day, and this underestimation increases with increasing rainfall depth. Similarly for HSC module, if A_s is determined by S_u/S_{uMax} at the beginning of a day, the effect of P_e on runoff coefficient is not considered.

Reply: The influence of S_{uMax}/P_e on runoff coefficient estimation (Moore, 1985; Wang, 2018) has been discussed in the second paragraph of Section 6.3.

2. For HSC and HSC-MCT modules: the relationship $A_s=f(S_u/S_{uMax})$ is obtained from the HAND values (Figure 2d). This relationship can be obtained by fitting a distribution function to the CDF of normalized HAND values (e.g., Figure 2b). For example, if the distribution used in Xinanjiang (Zhao, 1992) and VIC (Wood et al., 1992) is applied, the CDF of storage capacity is:

$$F(C) = 1 - \left(1 - \frac{C}{C_m}\right)^\beta$$

The mean value of storage capacity is:

$$S_{uMax} = \frac{C_m}{\beta+1}$$

Substituting C_m from equation (2) into equation (1), we obtain

$$F(C) = 1 - \left(1 - \frac{1}{\beta+1} \frac{C}{S_{uMax}}\right)^\beta$$

c/S_{uMax} is the normalized HAND values (HAND values divided by its average) in Figure 2b. The value of β is estimated by fitting the distribution. Then the relationship $A_S=f(S_u/S_{uMax})$ is obtained:

$$A_S = 1 - \left(1 - \frac{S_u}{S_{uMax}}\right)^{\frac{\beta}{\beta+1}}$$

The curve for $A_S \sim S_u/S_{uMax}$ is concave since $\beta/(\beta+1) < 1$. $A_S \sim S_u/S_{uMax}$ for HBV is concave or convex. The distribution corresponding to the SCS curve number method is another alternative (Wang, 2018), and the CDF is written as:

$$F(C) = 1 - \frac{1}{a} + \frac{\frac{C}{S_{uMax}} + 1 - a}{a \sqrt{\left(1 + \frac{C}{S_{uMax}}\right)^2 - 2a \frac{C}{S_{uMax}}}}$$

Where a is the shape parameter. The $A_S \sim S_u/S_{uMax}$ relation for equation (5) is:

$$A_S = 1 - \frac{1}{a} + \frac{\frac{C}{S_{uMax}} + 1 - a}{a \sqrt{\left(1 + \frac{C}{S_{uMax}}\right)^2 - 2a \frac{C}{S_{uMax}}}}$$

$$\frac{C}{S_{uMax}} = \frac{\left(2 - a \frac{S_u}{S_{uMax}}\right) \frac{S_u}{S_{uMax}}}{2 \left(1 - \frac{S_u}{S_{uMax}}\right)}$$

Where **It is interesting to test the goodness-of-fit of these two distributions (equations 3 and 5) to the empirical $A_S \sim S_u/S_{uMax}$ from the HAND-based values.**

Reply: In the manuscript, we have compared the model performance of HSC and HSC-MCT with HBV and TOPMODEL (as benchmarks), and found that the HSC module performed better in both calibration and validation. HBV is a good benchmark, because it has a relatively straightforward way of representing the runoff threshold in the root zone, albeit by calibration. TOPMODEL is also a good benchmark, because it uses a topographical index to define the runoff threshold. In our approach, the spatial distribution of the HAND values is used to derive the spatial distribution of the runoff (connectivity) thresholds, but from another topographical perspective than TOPMODEL. We agree that it would be interesting to test the goodness-of-fit of the Cumulative Distribution Function (CDF) of HSC with not only the HBV, but also the Xinanjiang, GR4J and SCS models. However it might be worthwhile to clarify that the intention of this study is to propose a new runoff generation module (HSC), which is, to some extent, supported by large-sample ecological field observation, and free of calibration, rather than comparing the CDF of HSC with other existing modules. More details can be found in the second paragraph of Section 6.3.

3. Line 167: I guess that "SEF" represents "saturation excess flow". But spell out "SEF" which is not defined before. Same for SOF and SFF.

Reply: The full names of the SEF, and SOF have be clearly defined.

4. It may be good to add a map to show the spatial distribution of S_u .

Reply: The S_{uMax} for each MOPEX catchment in the HSC-MCT module was obtained in our previous study (Gao et al., 2014). We used the amount of root zone storage capacity, which ecosystems need to overcome drought periods (dry spells) with 20 years return period (S_{R20y}), as a proxy for S_{uMax} . The details of the method to derive the S_{R20y} can be found in Gao et al., 2014.

5. For figures with subplots, it is better to add “(a)” and “(b)”, e.g., Figure 7 and Figure 8.

Reply: Done

6. In the comparison of Figure 7a, is it possible to convert the distribution of TWI information to $A_s \sim S_u/S_{uMax}$ and add it to Figure 7a?

Reply: It is a good suggestion to put the TOPMODEL and HBV curves together, and compare their shape. But it is a difficult task, due to the different model assumption and concept. And to our best knowledge, we haven't found similar studies that systematically compare the TOPMODEL curves with HBV curves, which might indicate that this is not an easy task to be performed within a short time. Furthermore, in this study we just wanted to compare the model performance of HSC with HBV and TOPMODEL, rather than to unify all model approaches (see Section 6.3).

7. In Figure S4 (catchment 08171000), the calibrated β for HBV is about 1.8. $\beta = 1.35$ is very close to the curve of HSC. But it seems that the performance of HSC is better than HBV (lines 500-501 and Figure S3). Since β of HBV is calibrated, why is the calibrated value of β not around 1.35? Is this due to the effect of other calibrated parameters? Discussion on this may be helpful.

Reply: The effect of other calibrated parameters on model calibration and efficiency has been discussed in the third paragraph of Section 6.3.

8. This comment is related to the previous one. For the comparison between HSC and HSC-MCT, is the calibrated S_{uMax} for HSC similar to the estimated S_{uMax} by MCT method? How about the other calibrated parameters (e.g., D , K_f , K_s , T_{lag}) among the models (HBV, TOPMODEL HSC, and HSC-MCT)?

Reply: The comparison of the calibrated S_{uMax} and the estimated S_{uMax} by MCT can be found in Gao et al., 2014. For the other calibrated parameters, their effect on model performance will be discussed in the revised manuscript. It is worth noting that all models use the same model structure and prior range of remaining parameters (i.e. interception and response modules) to exclude the impact of other processes, and guarantee that the comparison of runoff generation modules is fair (see Section 2.4 and the third paragraph of Section 6.3).

References:

Moore, R. J. (1985), The probability-distributed principle and runoff production at point and basin scales, *Hydrol. Sci. J.*, 30, 273-297.

Wang, D.: A new probability density function for spatial distribution of soil water storage capacity leads to SCS curve number method, *Hydrol. Earth Syst. Sci. Discuss.*, <https://doi.org/10.5194/hess-2018-32>, in review, 2018.

Gao H, Hrachowitz M, Schymanski SJ, Fenicia F, Sriwongsitanon N, Savenije HHG. 2014. Climate controls how ecosystems size the root zone storage capacity at catchment scale. *Geophysical Research Letters* 41 (22): 7916–7923 DOI: 10.1002/2014gl061668

Replies to Anonymous Referee #2

This study proposed the HAND-based storage capacity curve (HSC) for runoff generation parameterization in hydrological models. I like the idea to provide parameter reduced modules for hydrological modeling, considering the significant uncertainty in parameter calibration. However, the benefits for reducing parameter uncertainty by the HSC module were not illustrated by the current results. The authors claimed that the HSC/HSC-MCT module possess higher robustness and bear the potential to be implemented in prediction of ungauged basins, which however are not convincing from the current results. The benefits of the HSC/HSC-MCT modules need to be further discussed.

Reply: We thank the Anonymous Referee #2 for the very constructive and detailed comments. For the benefits of HSC/HSC-MCT modules, we have added the results of model validation in the BB catchment (first paragraph of Section 4.2), and the model performance evaluated by I_{KGL} in the MOPEX catchments (first paragraph of Section 5.2). Moreover, the limitations of the two modules are also discussed in Section 6.3. Please find our point-by-point responses to your comments in below.

First, the HSC module obviously overestimated the saturated area fraction in the Bruntland Burn (BB) basin. The improvement for the correlation from 0.5 (TOPMODEL) to 0.6 (HSC) is rather small, which does not make any sense for illustrating the reduced deviations between the observed and simulated saturated area fractions. The model performance in validation period were not evaluated in the BB basin. Although the HSC module gained performance improvements on high flows in both calibration and validation periods in many MOPEX basins, the performance gains on low flows were not investigated. Moreover, the non-parameter HSC-MCT module produced much lower performance than the HSC module in many MOPEX cases. The gains for the HSC module should be attributed to the parameter calibration procedure, and potentially demonstrated the failure of the MCT module for many MOPEX cases.

Reply:

Overestimation of the saturated area. The overestimation of the saturated area is most likely caused by the different definitions of saturated areas used in field measurements (saturated soils connected to the stream network as detected by the “squishy boots method”) and in hydrological models (areas with potential for water accumulation across the catchment). The discussion and interpretation of the overestimation of the saturated area fraction in the BB basin are described in the third paragraph of Section 6.3. And we have further clarified the method to obtain experimental data in the second paragraph of Section 3.1.

Model validation in BB basin. We now have added the model performance for a validation period (2009-2014) and evaluated the models in the BB (see the first paragraph of Section 4.2).

Model performance on low flow. The performance gains on low flow (I_{KGL}) have been investigated and are shown in the supplementary figure S3. The results of I_{KGL} illustrate that our proposed modules (HSC and HSC-MCT) also performed better in low flow simulation.

Second, it is not fair to call the proposed modules are calibration-free. The HSC module also implied two parameters for the model application. The stream initiation threshold area was not included for

the model calibration, but was tested to calculate the HAND values. I guess this threshold area should be tested in calculation experiments to prepare the model results using the HSC modules. The effects of this parameter on the performance of the HSC modules were not investigated in the results. Including this parameter in the calibration procedure would most likely to improve the model performance. Moreover, model calibration procedures are required to determine the remaining parameter values in Table 1 for both the applications of HSC and HSC-MCT modules. The benefits to reduce parameter uncertainty by excluding one-two parameters by the HSC and HSC-MCT modules were not clear. Considering the preparation of HAND values using DEM dataset in the HSC and HSC-MCT modules, the computational cost should be much higher than the calibrated modules in HBV and TOPMODEL.

Reply:

Calibration-free. We may politely insist that the HSC-MCT is a calibration-free runoff generation module. We agree that the threshold area for stream initiation is important while generating HAND maps. But the threshold area can be determined based on observation rather than calibration, although the threshold area varies in different climate, geology and landscape classes. The limitation of the fixed threshold area has been discussed in the third paragraph of Section 6.3.

MCT method. MCT is an approach to estimate the S_{uMax} by measurable input. But since we fixed this parameter as S_{R20y} (the amount of root zone storage capacity, which ecosystems need to bridge droughts with 20 years return period), which may also vary in different ecosystems. Improving the MCT to allow more flexible estimation for different ecosystems will be promising to improve model performance, which is discussed in the first paragraph of Section 6.3.

Computational cost. The discussion on the computational cost has been added in the revised manuscript (see the third paragraph of Section 6.3).

Some other major concerns on the results are listed as follow.

1. Figure 6, why not show the saturated area fraction simulated by the HBV module? Is the HBV module spatially discretized for the model application?

Reply: The saturated area fraction simulated by HBV is presented in Figure 8b. But the HBV cannot explicitly generate the spatial discretization of saturation areas.

2. Figure 7, why was the beta value of 0.98 used for the HBV module? Was this beta value derived from the model calibration? Have you tried other beta values for the comparison between HBV and HSC modules? Why not show this curve for the TOPMODEL module? What is your purpose to show the frequency of TWI? Could you also show the frequency of HAND?

Reply: Yes, the beta value of 0.98 is the averaged calibrated value of beta. Please note that the intention of the HSC module is to propose a new runoff generation module, which is, to some extent, supported by large-sample ecological field observation, and free of calibration, rather than fitting the CDF of HSC with other existing curves/modules (see the second paragraph of Section 6.3). The purpose to show the TWI frequency of TOPMODEL is to demonstrate the curve that we used to estimate runoff in

TOPMODEL. The HSC curve in Figure 7 is derived from the spatial distribution of HAND, therefore the HAND distribution curve is not shown in this figure.

3. Figure 8, the label for soil moisture was missed. It is very difficult to find the observed soil moisture (or you don't have?). Can you label (a-b) for the two subplots? For the second and fourth events, the TOPMODEL matched the observed saturated area fractions very well. How to explain this? Please refine the caption, which is very difficult to understand.

Reply: We don't have the observed soil moisture data, but we have the data of observed saturated area proportion. Label a-b have been added in Figure 8, and the caption of Figure 8 has also been refined. TOPMODEL does perform better in the second and the fourth events, but generally HSC performs better than TOPMODEL (evaluated by R^2 and I_{KGE}) (Section 4.3).

4. Figure 9, as I suggested before, a correlation coefficient does not make any sense to illustrate the deviations between the observed and simulated saturated area fractions, given that only seven observation events. Could you use some other metrics to compare the bias or deviation errors between the observed and simulated saturated area fractions?

Reply: Thank you for the suggestion to use a different criteria to evaluate model performance to reproduce saturation areas. I_{KGE} might be a better metric to evaluate model performance on saturated area fraction estimation. Evaluated by I_{KGE} , HSC also performs better than the TOPMODEL, although both HSC and TOPMODEL do not perform well (-3.0 for HSC, and -3.4 for TOPMODEL). The reasons for the unsatisfactory results are discussed in the third paragraph of Section 6.3.

5. Figures 10-11, what do you intend to say from these figures?

Reply: We intended to present the procedures to derive the HSC curves for the MOPEX catchments, which we believe are helpful for readers to understand how the HSC module works.

6. Figure 12, I suggest to compare the values for I_{KGL} as well. The models were calibrated on both I_{KGL} and I_{KGE} , there should be strong trade-off between these two objective functions. That means the HSC module possibly sacrificed the performance for low flows (I_{KGL}) to improve the performance for high flows (I_{KGE}). The evaluated modules mainly differed on the calculation of soil storage capacity, which has significant effect on the generation of low flows. In my opinion, performance for low flows should also be an important indicator for the validity of the runoff generation assumptions.

Reply: The results of I_{KGL} have been incorporated into the revised manuscript (Figure S3, and the first paragraph of Section 5.2).

Minor concerns:

1. I suggest to remove "Calibration-free" from the title. HSC module needs to be calibrated, and the HSC-MCT module performed poorly in many MOPEX cases.

Reply: We may politely insist that the HSC-MCT module is calibration-free and performs equally well or better as a calibrated model. There are two reasons. Firstly, as we clarified in the above, HSC is directly derived from the HAND distribution in a DEM, without any calibration. Secondly, HSC-MCT performs comparably well with HBV. Since the median I_{KGE} value of HSC-MCT is 0.65, which is a better performance compared to HBV (0.61). And the averaged I_{KGE} value of HSC-MCT is 0.59, which is comparable to 0.62 (HBV). The models' performance on I_{KGL} have similar results. So, it is fair to say the model performance of the calibration-free HSC-MCT and HBV are comparable.

2. Lines 30-33, I am not convinced to agree with this from the current results. What do you mean “facilitated effective visualization of the saturated area”? Is it important?

Reply: This sentence has been rephrased.

3. Introduction is too long from my taste. It is very difficult to get the motivations of this study from this section. I would suggest to refine it.

Reply: We have tremendously refined and shortened the introduction.

4. Lines 213-214, remove “Hydrological: : inevitable”. Line 217, what do you mean “HAND contours are parallel in runoff generation”? Is that possible derived from the DEM?

Reply: This have been rephrased.

5. Line 227, could you please add more details for the calculation of HAND values?

Reply: This has been rephrased. And more details about the calculation of HAND can be found in Rennó et al., 2008; Gharari et al., 2011.

6. Line 314, how did you define the pareto-frontier? Did you use the Euclidean distance or threshold values?

Reply: The Pareto frontier is defined by Euclidean distance. Please refer to Vrugt et al., 2003.

7. Section 3.1, could you please add some details on the climatic and hydrological data in the BB basin? Any ground gauged stations do you have there?

Reply: Yes, we have added more but brief details on the climatic and hydrological data in the BB catchment.

8. Also in section 3.1, could you introduce the spatial interpolation of the field mapping of the saturated areas?

Reply: The saturation maps are not interpolated. They are generated directly by field mapping, and global positioning system (GPS) was used to delineate the boundary of saturation areas using the “squishy boot method” (Ali et al., 2014; Birkel et al., 2010). We have clarified this in the methods of the revised manuscript.

9. Line 369-374, move to the methodology section.

Reply: We have revised as suggested.

10. Lines 415-420, move to the methodology section.

Reply: We have revised as suggested.

11. Lines 455-456, ‘dramatically improved’ may be not fair. ‘simultaneously maintaining model robustness and consistency’ is also not convinced by the results.

Reply: We have revised as suggested.

12. Lines 491-496, it is not fair to only discuss the cases where HSC/HSC-MCT outperformed the benchmark modules. Why not discuss the reasons for the cases where HSC/HSC-MCT produced lower performance?

Reply: The results and the reasons for the cases where HSC/HSC-MCT produced lower performance have been described in the end of third and four paragraphs of Section 5.2, and the end of the first paragraph of Section 6.1.

13. Discussion is also too much. It is difficult to get the main messages from the long text. Maybe remove lines 508-522, and lines 539-556.

Reply: We have revised as suggested.

14. Lines 646-647, maybe it is not so important to say as one of the conclusions here.

Reply: We have revised as suggested.

15. There are many sentence started with ‘And’, this is very strange (kind of grammatical error).

Reply: We have revised the content thoroughly as suggested.

References:

Renno, C. D., Nobre, A. D., Cuartas, L. A., Soares, J. V., Hodnett, M. G., Tomasella, J., and Waterloo, M. J.: HAND, a new terrain descriptor using SRTM-DEM: Mapping terra-firme rainforest environments in Amazonia, *Remote Sens. Environ.*, 112, 3469–3481, doi:10.1016/j.rse.2008.03.018, 2008.

Gharari, S., Hrachowitz, M., Fenicia, F., and Savenije, H. H. G.: Hydrological landscape classification: investigating the performance of HAND based landscape classifications in a central European meso-scale catchment, *Hydrol. Earth Syst. Sci.*, 15, 275–3291, doi:10.5194/hess-15-3275-2011, 2011

Vrugt, J. A., Gupta, H. V., Bastidas, L. A., Bouten, W., and Sorooshian, S.: Effective and efficient algorithm for multiobjective optimization of hydrologic models, *Water Resour. Res.*, 39, 1214, doi:10.1029/2002wr001746, 2003.

Ali, G., Christian Birkel, Doerthe Tetzlaff, et al. A comparison of wetness indices for the prediction of observed connected saturated areas under contrasting conditions[J]. *Earth Surface Processes and Landforms*, 2014, 39(3):399-413.

Birkel, C., Tetzlaff, D., Dunn, S. M. and Soulsby, C. (2010), Towards a simple dynamic process conceptualization in rainfall–runoff models using multi-criteria calibration and tracers in temperate, upland catchments. *Hydrol. Process.*, 24: 260-275. doi:[10.1002/hyp.7478](https://doi.org/10.1002/hyp.7478)

Replies to Anonymous Referee #3

General comments

This study presents a new concept for runoff generation description in conceptual hydrologic models. The new approach is based on HAND (height above nearest drainage) information derived from digital elevation model. The methodology is tested for two cases: (1) small experimental catchment in Scotland; (b) MOPEX dataset in the US. Results are compared against observed saturation patterns (in case 1) and discharge observations (both cases), as well against simulations of two other conceptual hydrologic models. The authors conclude that the new concept compares well with other two calibrated models and allows to describe spatial distribution of the root zone storage capacity.

Overall the topic is interesting and within the scope of HESS. However I fully agree with referee #2 that manuscript will benefit from some strengthening of the take home message, i.e. by providing more thorough and additional process based evaluation of results. I missed some more thorough process based interpretation of the reasons for similarity/differences in saturated area patterns for case 1 (catchment in Scotland). It seems to me that the differences between observed and simulated saturated area patterns are quite large and does not support well the interpretation that the new concept is better than the other approaches (yes, it is a little bit better than the models but for some days quite far from the observations and not convincing well the benefits of the proposed approach). The results for case 2 (MOPEX dataset) present mostly a statistical comparison of efficiency numbers (average, median), but does not tell much about the seasonal, geological, vegetation, climate and flow characteristics impacts on the efficiency evaluation. Some classification of catchments according e.g. similar TWI or HAND based indices, runoff regime indices, etc. and subsequent separate analysis of results for such groups will allow to more clearly indicate the role of different physiographic conditions on the results. I'm not sure to what extent can be the presented example for one catchment generalised for the other catchments, so some more assessment will be useful here. For example the results indicate that the new concept is better for mild sloped catchments, so a figure showing the results for all such catchments compared to the others will be interesting. Along the same line, similar evaluation for different geological/vegetation/climate groups of catchments with some process based interpretation of results will shed more light about what new and different information is obtained in the new HAND based storage capacity estimates compared to TWI (research question 2). (I'm missing a clear answer here - the maps are quite difficult to read, particularly for people which are not experts on the local situation). The discussion of the results is in some parts too vague and not linked well with the results (e.g. section 6.2). On the other hand there are much more MOPEX based studies and some of them indicate better model performance (e.g. for HBV model, e.g. Kollat et al, 2012, <https://doi.org/10.1029/2011WR011534>) than found here. So, some more thorough link with existing MOPEX studies will be thus suggested.

Replies:

We thank Anonymous Referee #3 for all his/her constructive comments and useful suggestions. For the benefits of HSC/HSC-MCT modules, we have added the results of model validation in the BB catchment (first paragraph of Section 4.2), and the model performance evaluated by I_{KGL} in the MOPEX catchments

(first paragraph of Section 5.2). Moreover, the limitations of the two modules are also discussed in Section 6.3. Please find our point-by-point responses to your comments in below.

1. *Overestimation of the saturated area.* The overestimation of the saturated area is most likely caused by the different definitions of saturated areas used in field measurements (saturated soils connected to the stream network as detected by the “squishy boots method”) and in hydrological models (areas with potential for water accumulation across the catchment). The discussion and interpretation of the overestimation of the saturated area fraction in the BB basin are described in the third paragraph of Section 6.3. And we have further clarify the method to obtain experimental data in the second paragraph of Section 3.1.
2. *Testing the impact of seasonal, geological, vegetation, climate and flow characteristics on model efficiency.* Actually, we have conducted a study with the MOPEX data to test the impact of vegetation, climate, geology, topography, and other catchment characteristics on the shape of the beta function, and found that the topographic information has the most significant impact on the shape of beta function (Gao et al., 2018). It is found that the topographic information has the most significant impact on the shape of beta function. Therefore, we merely investigated the impact of topography on beta function and model efficiency in this study (see the last paragraph in Section 6.1).
3. The discussion has been revised to be better linked with the results.
4. We compared the HBV model performance in MOPEX catchments with other studies (e.g. Ye et al., 2014). We will also refer to Kollat et al. (2012) in the revised manuscript.

Specific comments

1) Abstract: Please consider to be more specific about how much better the HSC concept is in reproducing the spatio-temporal pattern of the observed saturation areas, as well as in comparison with calibration and validation efficiencies of other conceptual models.

Reply: We have rephrased the last sentence in the Abstract.

2) Figure 1 and associated text. I wonder to what extent the new concept (HAND is proportional to storage capacity) reflects different geomorphological and geological processes? In which geological conditions one can apply the concept?

Reply: Topography, with fractal characteristic, is often the dominant driver of runoff, as well as being a good integrated indicator for vegetation cover, rooting depth, root zone evaporation and transpiration deficits, soil properties, and even geology. But quantifying to what extent the HSC concept reflects different geomorphological and geological processes is still a challenge (Rempe and Dietrich, 2014; Gomes, 2016), which needs further investigation. Please see the second paragraph of Section 6.3.

3) Figure 6. The colour legends are very confusing. It will be easier to have the same legend for all maps.

Reply: I have replot Figure 6, to make sure they have the same legend for all maps.

4) It will be interesting to provide, as a supplement, a list of used catchments with the results.

Reply: A list of the used catchments has been added as SI material.

References:

Gao, H., Duan, Z., Cai, H. (2018) Understand the impacts of landscape features on the shape of storage capacity curve and its influence on flood, *Hydrology Research*, 49(1): 90-106.

Ye A, Duan Q, Yuan X, Wood EF, Schaake J. 2014. Hydrologic post-processing of MOPEX streamflow simulations. *Journal of Hydrology* 508: 147–156 DOI: 10.1016/j.jhydrol.2013.10.055

Kollat, J. B., P. M. Reed, and T. Wagener. "When are multiobjective calibration trade - offs in hydrologic models meaningful?." *Water Resources Research* 48.3(2012):3520.

Rempe, D. M., and W. E. Dietrich (2014), A bottom-up control on fresh-bedrock topography under landscapes, *Proc. Natl. Acad. Sci. U. S. A.*, 111(18), 6576–6581, doi:10.1073/pnas.1404763111.

Gomes GJC, Vrugt JA, Vargas EA. 2016. Toward improved prediction of the bedrock depth underneath hillslopes: Bayesian inference of the bottom-up control hypothesis using high-resolution topographic data. *Water Resources Research* 52 (4): 3085–3112

1 A simple topography-driven and 2 calibration-free runoff generation module

3 Hongkai Gao^{1,2,3*}, Christian Birkel^{4,5}, Markus Hrachowitz⁶, Doerthe Tetzlaff⁵, Chris Soulsby⁵, Hubert H. G. Savenije⁶

4
5 ¹ Key Laboratory of Geographic Information Science (Ministry of Education of China), East China Normal University,
6 Shanghai, China.

7 ² School of Geographical Sciences, East China Normal University, Shanghai, China.

8 ³ Julie Ann Wrigley Global Institute of Sustainability, Arizona State University PO Box 875402. Tempe, AZ 85287-5402.

9 ⁴ Department of Geography, University of Costa Rica, San José, Costa Rica

10 ⁵ Northern Rivers Institute, University of Aberdeen, Scotland.

11 ⁶ Water Resources Section, Delft University of Technology, Delft, Netherlands.

12
13 *Corresponding to Hongkai Gao (hkgao@geo.ecnu.edu.cn)

15 Abstract

16 Reading landscapes and developing calibration-free runoff generation models that adequately reflect land
17 surface heterogeneities remains the focus of much hydrological research. In this study, we report a novel
18 and simple topography-driven runoff generation parameterization – the HAND-based Storage Capacity
19 curve (HSC), that uses a topographic index (HAND, Height Above the Nearest Drainage) to identify
20 hydrological similarity and the extent of saturated areas in catchments. The HSC can be used as a module
21 in any conceptual rainfall-runoff model. Further, coupling the HSC parameterization with the Mass Curve
22 Technique (MCT) to estimate root zone storage capacity (S_{uMax}), we developed a calibration-free runoff
23 generation module HSC-MCT. The runoff generation modules of HBV and TOPMODEL were used for
24 comparison purposes. The performance of these two modules (HSC and HSC-MCT) was first checked
25 against the data-rich Bruntland Burn (BB) catchment in Scotland, which has a long time series of field-
26 mapped saturation area extent. We found that the HSC performed better in reproducing the spatio-
27 temporal pattern of the observed saturated areas in the BB compared to TOPMODEL. The HSC and HSC-
28 MCT modules were subsequently tested for 323 MOPEX catchments in the US, with diverse climate, soil,

1 vegetation and geological characteristics. Comparing with HBV and TOPMODEL, the HSC performs better
2 in both calibration and validation. Despite having no calibrated parameters, the HSC-MCT module
3 performed comparably well with calibrated modules, highlighting the robustness of the HSC
4 parameterization to describe the spatial distribution of the root zone storage capacity and the efficiency
5 of the MCT method to estimate S_{uMax} . Moreover, the HSC-MCT module facilitated ~~effective~~ visualization
6 of the saturated area, which has the potential to be used for broader hydrological, ecological,
7 climatological, geomorphological, and biogeochemical studies.

8

9 1 Introduction

10 Determining the volume and timing of runoff generation from rainfall inputs remains a central challenge
11 in rainfall-runoff modelling (Beven, 2012; McDonnell, 2013). Creating a simple, calibration-free, but robust
12 runoff generation module has been, and continues to be, an essential pursuit of hydrological modellers.
13 Although we have made tremendous advances to enhance our ability on Prediction in Ungauged Basins
14 (PUB) (Sivapalan et al., 2003; Blöschl et al., 2013; Hrachowitz et al., 2013; Hrachowitz et al., 2013), it is not
15 uncommon that models become increasingly complicated in order to capture the details of hydrological
16 processes shown by empirical studies (McDonnell, 2007; Sivapalan, 2009). More detailed process
17 conceptualization normally demands higher data requirements than our standard climatological and
18 hydrological networks can provide, leading to more calibrated parameters and a probable increase in
19 model uncertainty (Sivapalan, 2009).

20 Hydrological connectivity is a key characteristic of catchment functioning, controlling runoff generation.
21 It is a property emerging at larger scales, describing the temporal dynamics of how spatially
22 heterogeneous storage thresholds in different parts of catchments are exceeded to contribute to storm
23 runoff generation and how they are thus “connected to the stream” (e.g. Zehe and Blöschl, 2004;
24 Bracken and Croke, 2007; Lehmann et al., 2007; Zehe and Sivapalan, 2009; Ali et al., 2013; Blume and
25 van Meerveld, 2015). Connectivity is controlled by a multitude of factors (Ali and Roy, 2010), including
26 but not limited to surface (e.g. Jencso et al., 2009) and subsurface topography (e.g. Tromp-van Meerveld
27 and McDonnell, 2006), soils (including preferential flow networks; e.g. Zehe et al., 2006; Weiler and
28 McDonnell, 2007) and land cover (e.g. Imeson and Prinsen, 2004; Jencso and McGlynn, 2011; Emanuel
29 et al., 2014) but also by the wetness state of the system (e.g. Detty and McGuire, 2010; Penna et al.,
30 2011; McMillan et al., 2014; Nippgen et al., 2015).

1 In detailed distributed hydrological bottom-up models, connectivity emerges from the interplay of
2 topography, soil type and water table depth. For example, TOPMODEL (Beven and Kirkby, 1979; Beven
3 and Freer, 2001) uses ~~the topographic-Topographic information w~~Wetness Index (TWI) to distinguish
4 hydrologic similarity; and SHE (Abbott et al. 1986) and tRIBS (Ivanov et al. 2004; Vivoni et al. 2005) use
5 partial differential equations to describe the water movement based on pressure gradients obtained by
6 topography; and the Representative Elementary Watershed (REW) approach divides catchment into a
7 number of REWs to build balance and constitutive equations for hydrological simulation (Reggiani et al.,
8 1999; Zhang and Savenije, 2005; Tian et al., 2008). As the relevant model parameters such as local
9 topographic slope and hydraulic conductivity can, in spite of several unresolved issues for example
10 relating to the differences in the observation and modelling scales (e.g. Beven, 1989; Zehe et al., 2014),
11 be obtained from direct observations, they could *in principle* be applied without calibration.

12 Zooming out to the macro-scale, top-down models, in contrast, are based on emergent functional
13 relationships that integrate system-internal heterogeneity (Sivapalan, 2005). These functional
14 relationships require parameters that are effective on the modelling scale and that can largely not be
15 directly determined with small-scale field observations (cf. Beven, 1995), ~~thus -Parameters in these~~
16 ~~models are therefore~~ traditionally determined by calibration. However, frequently the number of
17 observed variables for model calibration is, if available at all, limited to time series of stream flow. The
18 absence of more variables to constrain models results in such models being ill-posed inverse problems.
19 Equifinality in parameterization and in the choice of parameters then results in considerable model
20 uncertainty (e.g. Beven, 1993, 2006). To limit this problem and to also allow predictions in the vast
21 majority of ungauged catchments ~~worldwide that remain ungauged~~, it is therefore desirable to find
22 ways to directly infer effective model parameters at the modelling scale from readily available data
23 (Hrachowitz et al., 2013).

24 The component that is central for establishing connectivity in most top-down models is the soil moisture
25 routine. Briefly, it controls the dynamics of water storage and release in the unsaturated root zone and
26 partitions water into evaporative fluxes, groundwater recharge and fast lateral, storm flow generating
27 runoff. The latter of which is critical from the aspect of connectivity. In ~~majoritymost~~ regions, ~~where~~
28 Hortonian overland flow (HOF, i.e. infiltration excess overland flow) is of minor importance ~~(Dunne and~~
29 ~~Black, 1970; Sklash and Farvolden, 1979; Beven, 2004; Burt and McDonnell, 2015),~~ even in arid regions
30 where often most locally generated HOF is re-infiltrated while flowing on hillslopes (Liu et al., 2012) and
31 never reaches the stream channel network. Thus, the term saturation excess flow (SEF) ~~fast lateral flows~~

1 can represent, depending on the model and the area of application, different processes, such as
2 saturation overland flow, preferential flow, flow through shallow, high permeability soil layers or
3 combinations thereof. The interplay between water volumes that are stored and those that are released
4 laterally to the stream via fast, connected flow paths (“connectivity”) is in most top-down models
5 described by functions between water stored in the unsaturated root zone (“soil moisture”) and the
6 areal proportion of heterogeneous, local storage thresholds that are exceeded and thus “connected”
7 (Zhao et al., 1980). In other words, in those parts of a catchment where the storage threshold is
8 exceeded, ~~no more additional water can be stored and additional water input in these parts of the~~
9 ~~catchment will generate fast, lateral flows. This areal proportion of the catchment where thresholds are~~
10 ~~exceed, and~~ can alternatively be interpreted as runoff coefficient (e.g. Ponce and Hawkins, 1996; Perrin
11 and Andreassian, 2001; Fenicia et al., 2007; Bergström and Lindström, 2015). ~~Thus~~ ~~the~~ idea goes back
12 to the variable contributing area concept, assuming that only partial areas of a catchment, where soils
13 are saturated and thus storage thresholds are exceeded, contribute to runoff (Hewlett, 1961; Dunne and
14 Black, 1970; Hewlett and Troendle, 1975). Although originally developed for catchments dominated by
15 saturation overland flow, the extension of the concept to subsurface connectivity, posing that surface
16 and subsurface connectivity are “two sides of the same coin” (McDonnell, 2013), proved highly valuable
17 for models such as Xinanjiang (Zhao et al., 1980), HBV (Bergström and Forsman, 1973; Bergström and
18 Lindström, 2015), SCS-CN (Ponce and Hawkins, 1996; Bartlett et al., 2016), FLEX (Fenicia et al., 2008) ~~or~~
19 ~~and~~ GR4J (Perrin and Andreassian et al., 2001), ~~applied in other regions, too.~~

20 ~~In many top-down models, such as Xinanjiang or HBV. Among these models, connectivity is formulated in~~
21 ~~a general form as $C_R=f(S_U(t), S_{UMax}, \beta)$, where C_R is the runoff coefficient, i.e. the proportion of the~~
22 ~~catchment generating runoff, $S_U(t)$ is the catchment water content in the unsaturated root zone at any~~
23 ~~time t , S_{UMax} is a scale parameter representing the total storage capacity in the unsaturated root zone~~
24 ~~and β is a shape parameter, representing the spatial distribution of heterogeneous storage capacities in~~
25 ~~the unsaturated root zone. In a recent development, several studies suggest that S_{UMax} can be robustly~~
26 ~~and directly inferred long term water balance data, by the Mass Curve Technique (MCT), without the~~
27 ~~need for further calibration (Gao et al., 2014; de Boer-Euser et al., 2016; Nijzink et al., 2016). This leaves~~
28 ~~shape parameter β as only free calibration parameter for soil moisture routines of that form.~~

29 The parameters of these ~~storage-excess-distribution~~ functions are typically calibrated. In spite of being
30 the core component of soil moisture routines in many top-down models, little effort was previously
31 invested to find ways to determine the ~~shape of the functions describing the spatial heterogeneity of~~

1 ~~storage thresholds and thus connectivity pattern parameters~~ at the catchment-scale directly from
2 available data. An important step towards understanding and quantifying connectivity pattern directly
3 based on observations was recently achieved by intensive experimental work in the Tenderfoot Creek
4 catchments in Montana, US. In their work [Jencso et al. \(2009\)](#) were able to show that connectivity of
5 individual hillslopes in their headwater catchments is highly related to their respective upslope
6 accumulated areas. Using this close relationship, [Smith et al. \(2013\)](#) successfully developed a simple top-
7 down model with very limited need for calibration, emphasizing the value of “enforcing field-based
8 limits on model parameters” ([Smith et al., 2016](#)). Based on hydrological landscape analysis, [the FLEX-](#)
9 [Topo model \(Savenije, 2010\)](#) ~~can dramatically reduce the need for calibration (Gharari et al., 2014), and~~
10 ~~The model has also shown to hold considerable potential for spatial model transferability without the~~
11 ~~need for parameter re-calibration (Gao et al., 2014a; H. Gao et al., 2016).~~ [Savenije \(2010\)](#) suggested that
12 [as topographical features are frequently linked to distinct hydrological functional traits, they may](#)
13 [potentially be used to construct a conceptual catchment model based on a perceptual model of](#)
14 [hydrological units. Gharari et al., 2014 found that by imposing semi-quantitative relational constraints,](#)
15 ~~the FLEX-Topo model can dramatically reduce the need for calibration. The model has also shown to~~
16 ~~hold considerable potential for spatial model transferability without the need for parameter re-~~
17 ~~calibration (Gao et al., 2014a; H. Gao et al., 2016).~~ [In a recent development](#) [Recently, several studies](#)
18 [suggest that \$S_{uMax}\$ can be robustly and directly inferred from long-term water balance data using, by the](#)
19 [Mass Curve Technique \(MCT\), without the need for further calibration \(Gao et al., 2014; de Boer-Euser](#)
20 [et al., 2016; Nijzink et al., 2016\).](#) This leaves [the shape parameter \$\beta\$ as the only free calibration](#)
21 [parameter for soil moisture routines of that form.](#)

22 ~~In many top-down models, such as Xinanjiang or HBV, connectivity is formulated in a general form as~~
23 ~~$C_u = f(S_u(t), S_{uMax}, \beta)$, where C_u is the runoff coefficient, i.e. the proportion of the catchment generating~~
24 ~~runoff, $S_u(t)$ is the catchment water content in the unsaturated root zone at any time t , S_{uMax} is a scale~~
25 ~~parameter representing the total storage capacity in the unsaturated root zone and β is a shape~~
26 ~~parameter, representing the spatial distribution of heterogeneous storage capacities in the unsaturated~~
27 ~~root zone. In a recent development, several studies suggest that S_{uMax} can be robustly and directly~~
28 ~~inferred long term water balance data, by the Mass Curve Technique (MCT), without the need for~~
29 ~~further calibration (Gao et al., 2014; de Boer-Euser et al., 2016; Nijzink et al., 2016). This leaves shape~~
30 ~~parameter β as only free calibration parameter for soil moisture routines of that form.~~

1 Topography is often the dominant driver of water movement caused by prevailing hydraulic gradients.
2 More crucially, topography usually provides an integrating indicator for hydrological behavior, since
3 topography is usually closely related with other landscape elements, such as soil vegetation climate and
4 even geology (Seibert et al., 2007; Savenije, 2010; Rempe and Dietrich, 2014; Gao et al., 2014b; Maxwell
5 and Condon, 2016; Gomes, 2016). The Height Above the Nearest Drainage (HAND; Rennó et al., 2008;
6 Nobre et al., 2011; Gharari et al., 2011), which can be computed from readily available digital elevation
7 models (DEM), could potentially provide first order estimates of groundwater depth, as there is some
8 experimental evidence that with increasing HAND, groundwater depths similarly increase (e.g. Haria and
9 Shand, 2004; Martin et al., 2004; Molenat et al., 2005, 2008; Shand et al., 2005; Condon and Maxwell,
10 2015; Maxwell and Condon, 2016). HAND can be interpreted as a proxy of the hydraulic head and is thus
11 potentially more hydrologically informative than the topographic elevation above sea level (Nobre et al.,
12 2011). Compared with the ~~Topographic Wetness Index (TWI)~~ in TOPMODEL, HAND is an explicit measure
13 of a physical feature linking terrain to water ~~relative~~ related to the potential energy for local drainage
14 (Nobre et al., 2011). More interestingly, topographic structure emerges as a powerful force determining
15 rooting depth under a given climate or within a biome, revealed by ecological observations in global
16 scale (Fan et al., 2017). This leads us to think from ecological perspective to use the topographic
17 information as an indicator for root zone spatial distribution without calibrating the β , and coupling it
18 with the MCT method to estimate the S_{uMax} , eventually create a calibration-free runoff generation
19 module.

20 In this study we are therefore going to test the hypotheses that: (1) HAND can be linked to the spatial
21 distribution of storage capacities (~~β~~) and therefore can be used to develop a new runoff generation
22 module (HAND-based Storage Capacity curve, i.e. HSC); (2) the distribution of storage capacities
23 determined by HAND contains different information than the topographic wetness index; (3) the
24 ~~estimates of β HSC~~ together with water balance-based estimates of S_{uMax} (MCT method) allow the
25 formulation of calibration-free parameterizations of soil moisture routines in top-down models directly
26 based on observations. All these hypotheses will be tested firstly in a small data-rich experimental
27 catchment (the Bruntland Burn catchment in Scotland), and then apply the model to a wide range of larger
28 MOPEX catchments (~~MOPEX~~, Model Parameter Estimation Experiment).

29 This paper is structured as follows. In the Methods section, we describe two of our proposed modules, i.e.
30 HSC (HAND-based Storage Capacity curve) and HSC-MCT, and two benchmark models (HBV, TOPMODEL).
31 This section also includes the description of other modules (i.e. interception, evaporation and routing) in

1 rainfall-runoff modelling, and the methods for model evaluation, calibration and validation. The Dataset
2 section reviews the empirically-based knowledge of the Bruntland Burn catchment in Scotland and the
3 hydrometeorological and topographic datasets of MOPEX catchments in the US for model comparison. The
4 Results section presents the model comparison results. The Discussion section interprets the relation
5 between rainfall-runoff processes and topography, catchment heterogeneity and simple model, and the
6 implications and limitations of our proposed modules. The conclusions are briefly reviewed in the
7 Summary and Conclusions section.

8 2 Methods

9 Based on our perceptual model that [saturation excess flow \(SEF\)](#) is the dominant runoff generation
10 mechanism in most cases, we developed the HAND-based Storage Capacity curve (HSC) module.
11 Subsequently, estimating the parameter of root zone storage capacity (S_{uMax}) by the [Mass Curve](#)
12 [Techniques \(MCT method\)](#) without calibration, the HSC-MCT was developed. In order to assess the
13 performance of our proposed modules, two widely-used runoff generation modules, i.e. HBV power
14 function and TOPMODEL module, were set as benchmarks. Other modules, i.e. interception, evaporation
15 and routing, are kept with identical structure and parameterization for the four rainfall-runoff models
16 (HBV, TOPMODEL, HSC, HSC-MCT, whose names are from their runoff generation modules), to
17 independently diagnose the difference among runoff generation modules ([Clark et al., 2008; 2010](#)).

18 2.1 Two benchmark modules

19 **HBV power function**

20 The HBV runoff generation module applies an empirical power function to estimate the nonlinear
21 relationship between the runoff coefficient and soil moisture ([Bergström and Forsman, 1973; Bergström](#)
22 [and Lindström, 2015](#)). The function is written as:

$$23 \quad A_s = \left(\frac{S_u}{S_{uMax}} \right)^\beta \quad (1)$$

24 Where A_s (-) represents the contributing area, which equals to the runoff coefficient of a certain rainfall
25 event; S_u (mm) represents the averaged root zone soil moisture; S_{uMax} (mm) is the averaged root zone
26 storage capacity of the studied catchment; β (-) is the parameter determining the shape of the power
27 function. The prior range of β can be from 0.1 to 5. The $S_u - A_s$ has a linear relation while β equals to 1. And
28 the shape becomes convex while the β is less than 1, and the shape turns to concave while the β is larger

1 than 1. In most situations, S_{uMax} and β are two free parameters, cannot be directly measured at the
2 catchment scale, and need to be calibrated based on observed rainfall-runoff data.

3 **TOPMODEL module**

4 The TOPMODEL assumes topographic information captures the runoff generation heterogeneity at
5 catchment scale, and the TWI is used as an index to identify rainfall-runoff similarity (Beven and Kirkby,
6 1979; Sivapalan et al., 1997). Areas with similar TWI values are regarded as possessing equal runoff
7 generation potential. More specifically, the areas with larger TWI values tend to be saturated first and
8 contribute to SEF; but the areas with lower TWI values need more water to reach saturation and generate
9 runoff. The equations are written as follow:

$$10 \quad D_i = \bar{D} + S_{uMax} (\bar{I}_{TW} - I_{TW_i}) \quad (2)$$

$$11 \quad \bar{D} = S_{uMax} - S_u \quad (3)$$

$$12 \quad A_s = \sum A_{s_i}; \quad \text{while } D_i < 0 \quad (4)$$

13 Where D_i (mm) is the local storage deficit below saturation at specific location (i); \bar{D} (mm) is the averaged
14 water deficit of the entire catchment (Equation 2), which equals to $(S_{uMax} - S_u)$, as shown in Equation 3. I_{TW_i}
15 is the local I_{TW} value. \bar{I}_{TW} is the averaged TWI of the entire catchment. Equation 2 means in a certain soil
16 moisture deficit condition for the entire catchment (\bar{D}), the soil moisture deficit of a specific location (D_i),
17 is determined by the catchment topography (I_{TW} and I_{TW_i}), and the root zone storage capacity (S_{uMax}).
18 Therefore, the areas with D_i less than zero are the saturated areas (A_{s_i}), equal to the contributing areas.
19 The integration of the A_{s_i} areas (A_s), as presented in Equation 4, is the runoff contributing area, which
20 equals to the runoff coefficient of that rainfall event.

21 Besides continuous rainfall-runoff calculation, Equations 2-4 also allow us to obtain the contributing area
22 (A_s) from the estimated relative soil moisture (S_u/S_{uMax}), and then map it back to the original TWI map,
23 which makes it possible to test the simulated contributing area by field measurement. It is worth
24 mentioning that the TOPMODEL in this study is a simplified version, and not identical to the original one,
25 which combines the saturated and unsaturated soil components.

1 2.2 HSC module

2 Hydrological models are human constructs that simplify the larger reality of hydrological processes
3 (Savenije, 2009), and assumptions are inevitable (Neuweiler and Helmig, 2017). In the HSC module this
4 study, we assume 1) SEF is the dominant runoff generation mechanism, while surface overland flow (SOF)
5 and subsurface flow (SSF) cannot be distinguished; 2) the local root zone storage capacity has a positive
6 and linear relationship with HAND, from which we can derive the spatial distribution of the root zone
7 storage capacity; 3) ~~HAND contours are parallel to each other in runoff generation. We believe that~~ rainfall
8 firstly feeds local soil moisture deficit, and no runoff can be generated before local soil moisture areas
9 being subsequently saturated and water moving downslope. And after being saturated and connected
10 with the channel network, either the cascade or parallel model structure does not impact on runoff
11 generation. So this parallel model structure not only simplifies our simulation, it is also very likely closer
12 to reality (Savenije, 2010).

13 Figure 1 shows the perceptual HSC module, in which we simplified the complicated 3-D topography of a
14 real catchment into a 2-D simplified hillslope. And then derive the distribution of root zone storage
15 capacity, based on topographic analysis and the second assumption as mentioned in the preceding
16 paragraph. Figure 2 shows the approach to derive the S_u - A_s relation, which are detailed as follows.

17 I. **Generate HAND map.** The HAND map ~~of study catchment, which represents the relative vertical~~
18 distance to the nearest river channel, can be generated from a Digital Elevation Model (DEM)
19 (Gharari et al., 2011). The stream initiation threshold area is a crucial parameter, determining the
20 perennial river channel network (Montgomery and Dietrich, 1989; Hooshyar et al., 2016), and
21 significantly impacting the HAND values. In this study, the start threshold area was chosen as 40ha
22 for the BB catchment to maintain a close correspondence with the observed stream network. And
23 for the MOPEX catchments, the stream initiation area threshold was set as 500 grid cells (4.05
24 km²), which falls in the range of previously reported stream initiation thresholds reported by
25 others (e.g. Colombo et al., 2007; Moussa, 2008, 2009). HAND maps were then calculated from
26 the elevation of each raster cell above the nearest grid cell flagged as a stream cell following the
27 flow direction (Gharari et al., 2011). The start area was chosen as 40ha to maintain a close
28 correspondence with observed stream network. The HAND map (Figure 10) was also generated
29 from the filled DEM, with the input of the flow direction and flow accumulation maps. Specifically,
30 the perennial river network was obtained, based on the flow accumulation map, by setting the
31 stream initiation area threshold of 500 grid cells (4.05 km²), which falls in the range of stream

initiation thresholds reported by others (e.g. Colombo et al., 2007; Moussa, 2008, 2009). In the end, HAND was then calculated from the elevation of each raster cell above nearest grid cell flagged as stream cell following the flow direction (Gharari et al., 2011).

II. **Generate normalized HAND distribution curve.** Firstly, sort the HAND values of grid cells in ascending order. Secondly, the sorted HAND values were evenly divided into n bands (e.g. 20 bands in this study), to make sure each HAND band has similar area. The averaged HAND value of each band is regarded as the HAND value of that band. Thirdly, normalize the HAND bands, and then plot the normalized HAND distribution curve (Figure 1b).

III. **Distribute S_{uMax} to each HAND band (S_{uMax_i}).** As assumed, the normalized storage capacity of each HAND band (S_{uMax_i}) increases with HAND value (Figure 1c). Based on this assumption, the unsaturated root zone storage capacity (S_{uMax}) can be distributed to each HAND band as S_{uMax_i} (Figure 2a). It is worth noting that S_{uMax} needs to be calibrated in the HSC module, but free of calibration in the HSC-MCT module.

IV. **Derive the $S_u - A_s$ curve.** With the number of s saturated HAND bands (Figure 2a-c), the soil moisture (S_u) can be obtained by Equation 5; and saturated area proportion (A_s) can be obtained by Equation 6.

$$S_u = \frac{1}{n} [\sum_{i=1}^s S_{uMax_i} + S_{uMax_s}(n - s)] \quad (5)$$

$$A_s = \frac{s}{n} \quad (6)$$

Where S_{uMax_s} is the maximum S_{uMax_i} of all the saturated HAND bands. Subsequently, the $A_s - S_u$ curve can be derived, and shown in Figure 2d.

The SEF mechanism assumes that runoff is only generated from the saturated areas~~generate runoff~~, therefore the proportion of saturation area is equal to the runoff coefficient of that rainfall-runoff event. Based on the $S_u - A_s$ curve in Figure 2d, generated runoff can be calculated from root zone moisture (S_u). The HSC module also allows us to map out the fluctuation of saturated areas by the simulated catchment average soil moisture. For each time step, the module can generate the simulated root zone moisture for the entire basin (S_u). Based on the $S_u - A_s$ relationship (Figure 2d), we can map S_u back to the saturated area proportion (A_s) and then visualize it in the original HAND map. Based on this conceptual model, we developed the computer program and created a procedural module. The technical roadmap can be found in Figure 3.

1 2.3 HSC-MCT module

2 The S_{uMax} is an essential parameter in various hydrological models (e.g. HBV, Xinanjiang, GR4J), which
3 determines the long-term partitioning of rainfall into infiltration and runoff. [Gao et al., 2014a](#) found that
4 S_{uMax} represents the adaption of ecosystems to local climate. Ecosystems may design their S_{uMax} based on
5 the precipitation pattern and ~~its~~[their](#) water demand. The storage is neither too small to ~~avoid~~[be](#) mortality
6 in dry seasons, nor too large to consume excessive energy and nutrients. Based on this assumption, we
7 can estimate the S_{uMax} without calibration, by the MCT method, from climatological and vegetation
8 information. More specifically, the average annual plant water demand in the dry season (S_R) is
9 determined by the water balance and the vegetation phenology, i.e. precipitation, runoff and seasonal
10 NDVI. Subsequently, based on the annual S_R , the Gumbel distribution ([Gumbel, 1935](#)), frequently used for
11 estimating hydrological extremes, was used to standardize the frequency of drought occurrence. S_{R20y} , i.e.
12 the root zone storage capacity required to overcome a drought once in 20 years, is used as the proxy for
13 S_{uMax} due to the assumption of a “cost” minimization strategy of plants as we mentioned above ([Milly,](#)
14 [1994](#)), and the fact that S_{R20y} has the best fit with S_{uMax} . [The \$S_{R20y}\$ of the MOPEX catchments can be found](#)
15 [in the map of](#) ~~{~~[Gao et al., \(2014a\)](#).

16 Eventually, with the MCT approach to estimate S_{uMax} and the HSC curve to represent the root zone storage
17 capacity spatial distribution, the HSC-MCT runoff generation module is created, without free parameters.
18 It is worth noting that both the HSC-MCT and HSC modules are based on the HAND derived S_u-A_s relation,
19 and their distinction lays in the methods to obtain S_{uMax} . So far, the HBV power function module has 2 free
20 parameters (S_{uMax} , β). While the TOPMODEL and the HSC both have one free parameter (S_{uMax}). Ultimately
21 the HSC-MCT has no free parameter.

22 2.4 Interception, evaporation and routing modules

23 Except for the runoff generation module in the root zone reservoir (S_{UR}), we need to consider other
24 processes, including interception (S_{IR}) before the S_{UR} module, evaporation from the S_{UR} and the response
25 routine (S_{FR} and S_{SR}) after runoff generation from S_{UR} (Figure 4). Precipitation is firstly intercepted by
26 vegetation canopies. In this study, the interception was estimated by a threshold parameter (S_{iMax}), set to
27 2 mm ([Gao et al., 2014a](#)), below which all precipitation will be intercepted and evaporated (Equation 9)
28 ([de Groen and Savenije, 2006](#)). For the S_{UR} reservoir, we can either use the HBV beta-function (Equation
29 12), the runoff generation module of TOPMODEL (Equation 2-4) or the HSC module (Section 2.3) to
30 partition precipitation into generated runoff (R_u) and infiltration. The actual evaporation (E_a) from the soil
31 equals to the potential evaporation (E_p), if S_u/S_{uMax} is above a threshold (C_e), where S_u is the soil moisture

1 and S_{uMax} is the catchment averaged storage capacity. And E_a linearly reduces with S_u/S_{uMax} , while S_u/S_{uMax}
 2 is below C_e (Equation 13). The E_p can be calculated by the Hargreaves equation (Hargreaves and Samani,
 3 1985), with maximum and minimum daily temperature as input. The generated runoff (R_u) is further split
 4 into two fluxes, including the flux to the fast response reservoir (R_f) and the flux to the slow response
 5 reservoir (R_s), by a splitter (D) (Equation 14, 15). The delayed time from rainfall peak to the flood peak is
 6 estimated by a convolution delay function, with a delay time of T_{lagF} . Subsequently, the fluxes into two
 7 different response reservoirs (S_{FR} and S_{SR}) were released by two linear equations between discharge and
 8 storage (Equation 19, 21), representing the fast response flow and the slow response flow mainly from
 9 groundwater reservoir. The two discharges (Q_f and Q_s) generated the simulated streamflow (Q_m). The
 10 model parameters are shown in Table 1, while the equations are given in Table 2. More detailed
 11 description of the model structure can be referred to [Gao et al., 2014b and 2016](#). It is worth underlining
 12 that the only difference among the benchmark HBV type, TOPMODEL type, the HSC and the HSC-MCT
 13 models is their runoff generation modules. Eventually, there are 7 free parameters in HBV model, 6 in
 14 TOPMODEL and HSC model, and 5 in the HSC-MCT model.

15 2.5 Model evaluation, calibration, validation and models comparison

16 Two objective functions were used to evaluate model performance, since multi-objective evaluation is a
 17 more robust approach to quantifying model performance with different criteria than a single one. The
 18 Kling-Gupta efficiency ([Gupta et al., 2009](#)) (I_{KGE}) was used as the criteria to evaluate model performance
 19 and as an objective function for calibration. The equation is written as:

$$20 \quad I_{KGE} = 1 - \sqrt{(r-1)^2 + (\alpha-1)^2 + (\varepsilon-1)^2} \quad (7)$$

21 Where r is the linear correlation coefficient between simulation and observation; α ($\alpha = \sigma_m / \sigma_o$) is a
 22 measure of relative variability in the simulated and observed values, where σ_m is the standard deviation
 23 of simulated streamflow, and σ_o is the standard deviation of observed streamflow; ε is the ratio between
 24 the average value of simulated and observed data. And the I_{KGL} (I_{KGE} of the logarithmic flows) ([Fencia et al., 2007; Gao et al., 2014b](#)) is used to evaluate the model performance on baseflow simulation. ~~Since the response module, determined the baseflow simulation and I_{KGL} is kept the same for all four models, thus only the I_{KGE} results are presented in the results.~~

28 A multi-objective parameter optimization algorithm (MOSCEM-UA) ([Vrugt et al., 2003](#)) was applied for
 29 the calibration. The parameter sets on the Pareto-frontier of the multi-objective optimization were

1 assumed to be the behavioral parameter sets and can equally represent model performance. The
2 averaged hydrograph obtained by all the behavioral parameter sets were regarded as the simulated result
3 of that catchment for further studies. The number of complexes in MOSCEM-UA were set as the number
4 of parameters (7 for HBV, 6 for TOPMODEL and the HSC model, and 5 for HSC-MCT model), and the
5 number of initial samples was set to 210 and a total number of 50000 model iterations for all the
6 catchment runs. For each catchment, the first half period of data was used for calibration, and the other
7 half was used to do validation.

8 In module comparison, we defined three categories: if the difference of I_{KGE} of model A and model B in
9 validation is less than 0.1, model A and B are regarded as “equally well”. If the I_{KGE} of model A is larger
10 than model B in validation by 0.1 or more, model A is regarded as outperforming model B. If the I_{KGE} of
11 model A is less than model B in validation by -0.1 or less, model B is regarded to outperform model A.

12 3 Dataset

13 3.1 The Bruntland Burn catchment

14 The 3.2 km² Bruntland Burn catchment (Figure 5), located in north-eastern Scotland, was used as a
15 benchmark study to test the models performance based on a rich data base of hydrological measurements.
16 The Bruntland Burn is a typical many-upland catchments in North West Europe (e.g. [Birkel et al., 2010](#)),
17 namely a combination of steep and rolling hillslopes and over-widened valley bottoms due to the glacial
18 legacy of this region. The valley bottom areas are covered by deep (in parts > 30m) glacial drift deposits
19 (e.g. till) containing a large amount of stored water superimposed on a relatively impermeable granitic
20 solid geology ([Soulsby et al., 2016](#)). Peat soils developed (> 1m deep) in these valley bottom areas, which
21 remain saturated throughout most of the year with a dominant near-surface runoff generation
22 mechanism delivering runoff quickly via micro-topographical flow pathways connected to the stream
23 network ([Soulsby et al., 2015](#)). Brown rankers, peaty rankers and peat soils are responsible for a flashy
24 hydrological regime driven by saturation excess overland flow, while humus iron podzols on the hillslopes
25 do not favor near-surface saturation but rather facilitate groundwater recharge through vertical water
26 movement ([Tetzlaff et al., 2014](#)). Land-use is dominated by heather moorland, with smaller areas of rough
27 grazing and forestry on the lower hillslopes. Its annual precipitation is 1059 mm, with the summer months
28 (May-August) generally being the driest ([Ali et al., 2013](#)). Snow makes up less than 10% of annual
29 precipitation and melts rapidly below 500m. The evapotranspiration is around 400 mm per year and
30 annual discharge around 659 mm. The daily precipitation, potential evaporation, and discharge range was

1 [measured from January 1 in 2008 to September 30 in 2014 from installed monitoring equipment \(further](#)
2 [details in Birkel et al., 2010\)](#). The data from January 1, 2008 to December 31, 2010 is used ~~as~~for model
3 [calibration, and the data from January 1, 2011 to September 30, 2014 is used as a model validation period.](#)

4 The LiDAR-derived DEM map with 2m resolution shows elevation ranging from 250m to 539m (Figure 5).
5 There are 7 saturation area maps (Figure 6) (May 2, July 2, August 4, September 3, October 1, November
6 26, in 2008, and January 21, in 2009), measured directly by [the “squishy boot” method and](#) field mapping
7 [\(Ali et al., 2013\)](#), ~~by with a and a~~ global positioning system (GPS), ~~was used~~ to delineate the boundary of
8 saturation areas [\(Birkel et al., 2010; Ali et al., 2013\)](#). These saturation area maps revealed a dynamic
9 behavior of expanding and contracting areas connected to the stream network that were used as a
10 benchmark test for the HSC module.

11 3.2 MOPEX dataset

12 The MOPEX dataset was collected for a hydrological model parameter estimation experiment [\(Duan et al.,](#)
13 [2006; Schaake et al., 2006\)](#), containing 438 catchments in the CONUS (Contiguous United States). The
14 dataset contains the daily precipitation, daily maximum and minimum air temperature, and daily
15 streamflow. The longest time series range from 1948 to 2003. 323 catchments were used in this study
16 [\(see the name list in SI\)](#), with areas between 67 and 10,329 km², and excluding the catchments with data
17 records <30 years, impacted by snowmelt or with extreme arid climate (aridity index $E_p/P > 2$). The daily
18 streamflow was used to calibrate the free parameters, and validate the models. The Digital Elevation
19 Model (DEM) of the CONUS in 90m resolution was download from the Earth Explorer of United States
20 Geological Survey (USGS, <http://earthexplorer.usgs.gov/>).

21 4 Results of the Bruntland Burn

22 4.1 Topography analysis

23 [The generated HAND map, derived also from the DEM, is shown in Figure 5, with HAND values ranging](#)
24 [from 0m to 234m. Based on the HAND map, we can derive the \$S_u-A_s\$ curve \(Figure 7\) by analyzing the](#)
25 [HAND map with the method described in Section 2.3.](#) The TWI map of the BB (Figure 5) was generated
26 from [a 2m high-resolution LiDAR-derived](#) DEM. Overall, the TWI map, ranging from -0.4 to 23.4, mainly
27 differentiates the valley bottom areas with the highest TWI values from the steeper slopes. This [distinction](#)
28 [of landscape features is probably caused](#)supported by the fine resolution of the DEM ~~map in 2 m~~, since
29 previous research found the sensitivity of TWI to DEM resolution [\(Sørensen and Seibert, 2007\)](#). From the

1 TWI map, the frequency distribution function and the accumulative frequency distribution function can
2 be derived (Figure 7), with one unit of TWI as interval.

3 ~~The generated HAND map, derived also from the DEM, is shown in Figure 5, with HAND values ranging~~
4 ~~from 0m to 234m. Since HAND is sensitive to the definition of the perennial channel, which is highly~~
5 ~~impacted by the stream initiation threshold area (Montgomery and Dietrich, 1989; Gharari et al., 2011;~~
6 ~~Hooshyar et al., 2016). The start area was chosen as 40ha to maintain a close correspondence with~~
7 ~~observed stream network. Based on the HAND map, we can derive the S_u-A_s curve (Figure 7) by analyzing~~
8 ~~the HAND map with the method in Section 2.3.~~

9 4.2 Model performance

10 ~~The observed and simulated hydrographs of three models (HBV, TOPMODEL, and HSC) in 2008 are shown~~
11 ~~in Figure 8. We found that all the three models (HBV, TOPMODEL, and HSC) can perform well to~~
12 ~~reproduce the observed hydrograph (Figure 8). The I_{KGE} of the three models are all around 0.66 in~~
13 ~~calibration, which is largely in line with other studies from the BB (Birkel et al, 2010; 2014). And the~~
14 ~~calibrated I_{KGL} are 0.76, 0.72 and 0.74 for HSC, HBV and TOPMODEL, respectively in calibration. While in~~
15 ~~validation, the I_{KGE} of the three models are also around 0.66, while I_{KGL} are slightly~~
16 ~~lower with 0.75, 0.70 and 0.65 for the three models. Since the With measured rainfall-runoff time series~~
17 ~~only last from 2008 to 2014, which is too short to estimate the S_{R20y} (proxy for S_{uMax}) by MCT approach~~
18 ~~(which needs long-term hydro-meteorological observations data), the HSC-MCT model was not applied~~
19 ~~to the BB catchment.~~

20 The normalized relative soil moisture of the three model simulations are presented in Figure 8. Their
21 temporal fluctuation patterns are comparable. Nevertheless, the simulated soil moisture by TOPMODEL
22 has a larger variation, compared with HBV and HSC (Figure 8).

23 Figure 7 shows the calibrated power curve from HBV (averaged $\beta=0.98$) with the S_u-A_s curve obtained
24 from the HSC module. We found the two curves are largely comparable, especially while the relative soil
25 moisture is low. This result demonstrates that for the BB with glacial drift deposits and combined terrain
26 of steep and rolling hillslopes and over-widened valley bottoms, the HBV power curve can essentially be
27 derived from the S_u-A_s curve of the HSC module merely by topographic information without calibration.

28 4.3 Contributing area simulation

29 The observed saturation area and the simulated contributing area from both TOPMODEL and the HSC are
30 shown in Figure 6, 8, 9. We found although both modules overestimated the contributing areas, they can

1 capture the temporal variation. For example, the smallest saturated area both observed and simulated
2 occurred on July-02-2008, and the largest saturated area both occurred on January-21-2009.
3 Comparing the estimated contributing area of TOPMODEL with the HSC module, we found the results of
4 the HSC to better correlates better ($R^2=0.60$, $I_{KGE}=-3.0$) with the observed saturated areas than
5 TOPMODEL ($R^2=0.50$, $I_{KGE}=-3.4$) (Figure 9). For spatial patterns, the results of the HSC module are also more
6 closely comparable with the observed saturated areas than TOPMODEL (Figure 6). Based on these
7 results benchmarking the HSC module with observed saturated area maps, we proceeded to test HSC
8 for a wide range of climatically and geomorphologically different catchments across the US.

9 5 Results from the MOPEX catchments

10 5.1 Topography analysis of the Contiguous US and 323 MOPEX catchments

11 To delineate the TWI map for the CONUS, the depressions of the DEM were firstly filled with a threshold
12 height of 100m (recommended by Esri). ~~The slope map, i.e. the steepest local slope, was generated by the~~
13 ~~filled DEM, and the flow direction map was also derived from the filled DEM using the D8 algorithm~~
14 ~~(O'Callaghan and Mark, 1984; Jenson and Domingue, 1988). Subsequently, the flow accumulation map~~
15 ~~could be generated from the flow direction map. The accumulated upslope area (A), obtained from the~~
16 ~~flow accumulation map, was then divided by an estimate of the contour length (L), which is related to the~~
17 ~~flow direction map, to provide the local upslope area draining through a certain point per unit contour~~
18 ~~length ($a = A/L$). With the definition of TWI as $\ln(a/\tan \beta)$, the TWI map of the CONUS is produced (Figure~~
19 ~~S1). From Based on~~ the TWI map of the CONUS, we clipped the TWI maps for the 323 MOPEX catchments
20 with their catchment boundaries. And then the TWI frequency distribution and the accumulated
21 frequency distribution of the 323 MOPEX catchments (Figure S2), with one unit of TWI as interval, were
22 derived based on the 323 TWI maps.

~~The HAND map (Figure 10) was also generated from the filled DEM, with the input of the flow direction~~
24 ~~and flow accumulation maps. Specifically, the perennial river network was obtained, based on the flow~~
25 ~~accumulation map, by setting the stream initiation area threshold of 500 grid cells (4.05 km^2), which falls~~
26 ~~in the range of stream initiation thresholds reported by others (e.g. Colombo et al., 2007; Moussa, 2008,~~
27 ~~2009). In the end, HAND was then calculated from the elevation of each raster cell above nearest grid cell~~
28 ~~flagged as stream cell following the flow direction (Gharari et al., 2011).~~

29 In Figure 10, it is shown that the regions with large HAND values are located in the Rocky Mountains and
30 Appalachian Mountains, while the Great Plains has smaller HAND values. Interestingly, the Great Basin,

1 especially in the Salt Lake Desert, has small HAND values, illustrating its low elevation above the nearest
2 drainage, although their elevations above seas level are high. From the CONUS HAND map, we clipped the
3 HAND maps for the 323 MOPEX catchments with their catchment boundaries. We then plot their HAND-
4 area curves, following the procedures of [I and II-IV](#) in Section 2.2. Figure 11a shows the normalized HAND
5 profiles of the 323 catchments.

6 Based on the HAND profiles and the Step [V-III](#) in Section 2.2, we derived the normalized storage capacity
7 distribution for all catchments (Figure 11b). Subsequently, the root zone moisture and saturated area
8 relationship (A_s-S_u) can be plotted by the method in Step [V-IV](#) of Section 2.2. Lastly, reversing the curve of
9 A_s-S_u to S_u-A_s relation (Figure 11c), the latter one can be implemented to simulate runoff generation by
10 soil moisture. Figure 11c interestingly shows that in some catchments, there is almost no threshold
11 behavior between rainfall and runoff generation, where the catchments are covered by large areas with
12 low HAND values and limited storage capacity. Therefore, when rainfall occurs, wetlands response quickly
13 and generate runoff without a precipitation–discharge threshold relationship characteristic of areas with
14 higher moisture deficits. This is similar to the idea of FLEX-Topo where the storage capacity is distinguished
15 between wetlands and hillslopes, and on wetlands, with low storage capacity, where runoff response to
16 rainfall is almost instantaneous.

17 5.2 Model performance

18 Overall, the performance of the two benchmark models, i.e. HBV and TOPMODEL, for the MOPEX data
19 (Figure 12) is comparable with the previous model comparison experiments, conducted with four rainfall-
20 runoff models and four land surface parameterization schemes ([Duan et al., 2006](#); [Kollat et al., 2012](#); [Ye
21 et al., 2014](#)). The median value of I_{KGE} of the HBV type model is 0.61 for calibration in the 323 catchments
22 (Figure 12), and averaged I_{KGE} in calibration is 0.62. In validation, the median and averaged values of I_{KGE}
23 are kept the same as calibration. The comparable performance of models in calibration and validation
24 demonstrates the robustness of benchmark models and the parameter optimization algorithm (i.e.
25 MOSCEM-UA). The TOPMODEL improves the median value of I_{KGE} from 0.61 (HBV) to 0.67 in calibration,
26 and from 0.61 (HBV) to 0.67 in validation. But the averaged values of I_{KGE} for TOPMODEL are slightly
27 decreased from 0.62 (HBV) to 0.61 in both calibration and validation. The HSC module, by involving the
28 HAND topographic information without calibrating the β parameter, improves the median value of I_{KGE} to
29 0.68 for calibration and 0.67 for validation. The averaged values of I_{KGE} in both calibration and validation
30 are also increased to 0.65, comparing with HBV (0.62) and TOPMODEL (0.61). Furthermore, Figure 12
31 demonstrates that, comparing with the benchmark HBV and TOPMODEL, not only the median and

1 averaged values were improved by the HSC module, but also the 25th and 75th percentiles and the lower
2 whisker end, all have been ~~dramatically~~ improved. ~~The performance gains on baseflow (I_{KGL}) have been~~
3 ~~investigated and shown in the supplementary figure S3.~~ These results indicate the HSC module improved
4 ~~the model performance to reproduce hydrograph for both peak flow (I_{KGE}) and baseflow (I_{KGL}), and~~
5 ~~simultaneously maintaining model robustness and consistency.~~

6 Additionally, for ~~the HSC-MCT model,~~ the median I_{KGE} value, ~~the HSC-MCT leads to an is~~ improved
7 from 0.61 (HBV) to 0.65 in calibration, and from 0.61 (HBV) to 0.64 in validation, but ~~not as well~~
8 ~~performed lower compared to as~~ TOPMODEL (0.67 for calibration and validation). For the averaged I_{KGE}
9 values, they ~~were~~ slightly reduced from 0.62 (HBV) and 0.61 (TOPMODEL) to 0.59 for calibration and
10 validation. Although the HSC-MCT did not perform as well as the HSC module, considering there is no free
11 parameters to calibrate, the median I_{KGE} value of 0.64 (HBV is 0.61) and averaged I_{KGE} of 0.59 (TOPMODEL
12 is 0.61) are quite acceptable. In addition, the 25th and 75th percentiles and the lower whisker end of the
13 HSC-MCT model are all improved compared to the HBV model. Moreover, the largely comparable results
14 between the HSC and the HSC-MCT modules demonstrate the feasibility of the MCT method to obtain the
15 S_{UMax} parameter and the potential for HSC-MCT to be implemented in prediction of ungauged basins (~~PUB,~~
16 ~~cf. Sivapalan et al., 2003; Blöschl et al., 2013; Hrachowitz et al., 2013).~~ ~~Since the response routines~~
17 ~~determining the baseflow simulation of the four models are exactly the same, the results of I_{KGL} as an~~
18 ~~indicator to evaluate baseflow are not presented.~~

19 Figure 13 shows the spatial comparisons of the HSC and HSC-MCT models with the two benchmark models.
20 We found that the HSC performs “equally well” as HBV (the difference of I_{KGE} in validation ranges -0.1 ~
21 0.1) in 88% catchments, and in the remaining 12% of the catchments the HSC outperforms HBV (the
22 improvement of I_{KGE} in validation is larger than 0.1). In not a single catchment did the calibrated HBV
23 outperform the HSC. From the spatial comparison, we found that the catchments, where the HSC model
24 performed better are mostly located in the Great Plains, with modest sloping (4.0 degree), while the other
25 catchments have average slope of 8.1 degree. Comparing the HSC model with TOPMODEL, we found in
26 91% of the catchments that the two models have approximately equal performance. In 8% of the
27 catchments, the HSC model outperformed TOPMODEL. Only in 1% of the catchments (two in Appalachian
28 Mountain and one in the Rocky Mountain in California), TOPMODEL performed better. From spatial
29 analysis, we found the HSC outperformed catchments have flat terrain (2.3 degree) with moderate
30 averaged HAND value (26m), while the TOPMODEL outperformed catchments have steep hillslope (19
31 degree) with large averaged HAND value (154m).

1 Without calibration of S_{uMax} , as expected, the performance of HSC-MCT module slightly deteriorates
2 (Figure 12). In comparison with HBV, the outperformance reduced from 12% (HSC) to 4% (HSC-MCT), the
3 approximately equal-well simulated catchments dropped from 88% to 79%, and the inferior performance
4 increased from 0% to 17%. Also, in comparison with TOPMODEL, the better performance dropped from
5 8% (HSC model) to 7% (HSC-MCT model), the approximately equal catchments reduced from 91% to 72%,
6 and the inferior performance increased from 1% to 21%. The inferiority of the HSC-MCT model is probably
7 caused by the uncertainty of the MCT method for different ecosystems which have different survival
8 strategies and use different return periods to bridge critical drought periods. By using ecosystem
9 dependent return periods, this problem could be reduced (Wang-Erlandsson et al., 2016).

10 To further explore the reason for the better performance of the HSC approach, we selected the 08171000
11 catchment in Texas (Figure 13), in which both the HSC module and the HSC-MCT module outperformed
12 the two benchmark modules to reproduce the observed hydrograph (Figure S3S4). The HBV model
13 dramatically underestimated the peak flows, with I_{KGE} as 0.54, while TOPMODEL significantly
14 overestimated the peak flows, with I_{KGE} as 0.30. The HSC-MCT model improved the I_{KGE} to 0.71, and the
15 HSC model further enhanced I_{KGE} to 0.74.

16 Since the modules of interception, evaporation and routing are identical for the four models, the runoff
17 generation modules are the key to understand the difference in model performance. Figure S4-S5 shows
18 the HBV β curve and the S_u-A_s curve of the HSC model, as well the TWI frequency distribution. We found
19 that with a given S_u/S_{uMax} , the HBV β function generates less contributing area than the HSC model, which
20 explains the underestimation of the HBV model. In contrast, TOPMODEL has a sharp and steep
21 accumulated TWI frequency curve. In particular, the region with TWI=8 accounts for 40% of the catchment
22 area, and over 95% of the catchment areas are within the TWI ranging from 6 to 12. This indicates that
23 even with low soil moisture content (S_u/S_{uMax}), the contributing area by TOPMODEL is relatively large,
24 leading to the sharply increased peak flows for all rainfall events.

25 6 Discussion

26 6.1 Rainfall-runoff processes and topography

27 ~~In hillslope and catchment hydrology, the partitioning of precipitation into runoff and evaporation is a~~
28 ~~fundamental function in virtually all hydrological models. Bucket-type models (e.g. HBV and Xinanjiang),~~
29 ~~as one of the most widely used group of conceptual models, typically adopt two parameters to determine~~
30 ~~runoff generation. One is the root zone storage capacity (S_{uMax}) and the other is the shape parameter (i.e.~~

~~β) determining the relation between root zone moisture and runoff generation. In long term water balance studies, climate plays a key role in determining the storage capacity and the partition between evaporation and runoff (Budyko, 1971; Wang and Tang, 2014; Gao et al., 2014a). But for specific events, the key question is how antecedent soil moisture impacts runoff generation. Field studies support that in many mildly sloping catchments, SEF is the dominant runoff generation mechanism (Sklash and Farvolden, 1979; Burt and McDonnell, 2015). Therefore, it is essential to determine the temporal variability of the saturated area (equal to the contributing area and the runoff coefficient of a specific rainfall runoff event), to calculate runoff generation. Linking the runoff contributing area to topography is not a new insight in rainfall runoff modelling. TOPMODEL is an elegant pioneering model allowing us to understand the interaction between topography and connectivity. In this study, the HSC module uses a relatively new topographic index (i.e. HAND) to identify hydrological similarity.~~

We applied a novel approach to derive the relationship between soil moisture storage and the saturated area from HAND. The areas with relatively low HAND values are saturated earlier than areas with higher HAND values, due to the larger storage capacity in high HAND locations. The outperformance of the HSC model over the benchmark HBV and TOPMODEL in modestly sloping catchments indicates that the HSC module [likely](#) has a higher realism than the calibrated beta-function of the HBV model and the TWI of TOPMODEL in these regions. Very interestingly, [Fan et al., \(2017\)](#) presented a global synthesis of 2,200 root observations of >1000 species, and revealed the systematic variation of rooting depth along HAND (Fig.1, in [Fan et al., 2017](#)). Since rooting depth can be translated to root zone storage capacity through combination with soil plant-available water ([Wang-Erlandsson et al., 2016](#)). This large sample dataset, from ecological perspective, provides a strong support for the assumption of the HSC model on modest slopes, i.e. the increase of root zone storage capacity with HAND. More interestingly, on excessively drained uplands, rooting depth does not follow the same [role pattern](#), with shallow depth and limited to rain infiltration (Fig.1, in [Fan et al., 2017](#)). This could explain the inferior performance of HSC model to TOPMODEL in three MOPEX catchments (averaged HAND is 154 m) with excessively drained uplands, where Hortonian overland flow is likely the dominant mechanism, and the HSC assumption likely does not work well.

The FLEX-Topo model ([Savenije, 2010](#)) also uses HAND information as a topographic index to distinguish between landscape-related runoff processes, and has both similarity and differences with the HSC model. The results of the HSC model illustrate that the riparian areas are more prone to be saturated, which is consistent with the concept of the FLEX-Topo model. Another important similarity of the two models is

1 their parallel model structure. ~~From our perspective, the parallel model structure is closer to reality. Since~~
2 ~~before saturation, rainfall is firstly infiltrated into local storage, and water moves vertically; only after a~~
3 ~~certain level of saturation, water starts to move laterally. But~~ in both models it is assumed that the
4 upslope area has larger storage capacity, therefore the upper land generates runoff less and later than
5 the lower land. In other words, in most cases, the local storage is saturated due to the local rainfall, instead
6 of flow from upslope. ~~Therefore, the local storage is an essential feature, to estimate the saturated area~~
7 ~~and runoff generation, rather than the water coming from uphill.~~

8 The most obvious difference between the HSC and the FLEX-Topo ~~models~~ is the approach towards
9 discretization of a catchment. The FLEX-Topo model classifies a catchment into various landscapes, e.g.
10 wetlands, hillslopes and plateau. This discretization method requires threshold values to classify
11 landscapes, i.e. threshold values of HAND and slope, which leads to fixed and time-independent
12 proportions of landscapes. The HSC model does not require landscape classification, which reduced the
13 subjectivity in discretization and restricted the model complexity, as well as simultaneously allowing the
14 fluctuation of saturated areas (termed as wetlands in FLEX-Topo).

15 Except for topography, it is also interesting to test the impact of climate, geological, vegetation, and flow
16 characteristics on model efficiency. Gao et al., (2018) have conducted a study with the MOPEX dataset to
17 test the impact of various catchment characteristics on the shape of the beta function, and found that the
18 topographic information has the most significant impact on the shape of beta function. Therefore, we
19 merely investigated the impact of topography on beta function and model efficiency in this study.

20 6.2 Catchment heterogeneity and simple models

21 Catchments exhibit a wide array of heterogeneity and complexity with spatial and temporal variations of
22 landscape characteristics and climate inputs. For example, the Darcy-Richards equation approach is often
23 consistent with point-scale measurements of matrix flow, but not for preferential flow caused by roots,
24 soil fauna and even cracks and fissures (Beven and Germann, 1982; Zehe and Fluehler, 2001; Weiler and
25 McDonnell, 2007). As a result, field experimentalists continue to characterize and catalogue a variety of
26 runoff processes, and hydrological and land surface modelers are developing more and more complicated
27 models to involve the increasingly detailed processes (McDonnell et al., 2007). However, there is still no
28 compelling evidence to support the outperformance of sophisticated “physically-based” models in terms
29 of higher equifinality and uncertainty than the simple lumped or semi-distributed conceptual models in
30 rainfall-runoff simulation (Beven, 1989; Orth et al., 2015).

1 But evidence is mounting that a catchment is not a random assemblage of different heterogeneous parts
2 (Sivapalan, 2009; Troch et al., 2013; Zehe et al., 2013), and conceptualising heterogeneities does not
3 require complex laws (Chase, 1992; Passalacqua et al., 2015). Asking questions of “why” rather than “what”
4 likely leads to more useful insights and a new way forward (McDonnell et al., 2007). Catchment is a
5 geomorphological and even an ecological system whose parts are related to each other probably due to
6 catchment self-organization and evolution (Sivapalan and Blöschl, 2015; Savenije and Hrachowitz, 2017).
7 This encourages the hope that simplified concepts may be found adequate to describe and model the
8 operation of the basin runoff generation process. It is clear that topography, with fractal characteristic
9 (Rodriguez-Iturbe and Rinaldo, 1997), is often the dominant driver of runoff, as well as being a good
10 integrated indicator for vegetation cover (Gao et al., 2014b), rooting depth (Fan et al., 2017), root zone
11 evaporation and transpiration deficits (Maxwell and Condon, 2016), soil properties (Seibert et al., 2007),
12 and even geology (Rempe and Dietrich, 2014; Gomes, 2016). Therefore, we argue that increasingly
13 detailed topographic information is an excellent integrated indicator allowing modelers to continue
14 systematically represent heterogeneities and simultaneously reduce model complexity. The model
15 structure and ~~parametrization~~parameterization of both HSC and TOPMODEL are simple, but not over
16 simplified, as they capture probably the most dominant factor controlling runoff generation, i.e. the
17 spatial heterogeneity of storage capacity. Hence, this study also sheds light on the possibility of moving
18 beyond heterogeneity and process complexity (McDonnell et al., 2007), to simplify them into a succinct
19 and *a priori* curve by taking advantage of catchment self-organization probably caused by co-evolution or
20 the principle of maximum entropy production (Kleidon and Lorenz, 2004).

21 6.3 Implications and limitation

22 The calibration-free HSC-MCT runoff generation model may enhance our ability to predict runoff in
23 ungauged basins (Sivapalan et al., 2003; Blöschl et al., 2013; Hrachowitz et al., 2013). Hydrological models
24 still depend largely on observational data to feed statistical analysis and calibrate the free parameters.
25 This is probably not a major issue in the developed world, with abundant of comprehensive
26 measurements in many places, but for the developing world it requires prediction with sparse data and
27 fragmentary knowledge. Topographic information with high spatial resolution is freely available globally,
28 allowing us to implement the HSC model in global scale studies. In addition, thanks to the recent
29 development, testing, and validation of remote sensing evaporation products in large spatial scale (e.g.
30 Anderson et al., 2011; Hu and Jia, 2015), the S_{uMax} estimation has become possible without in situ hydro-

1 meteorological measurements (Wang-Erlandsson et al., 2016). These widely-accessible datasets make the
2 global-scale implementation of HSC-MCT module promising.

3 Although the new modules perform well in the BB and the MOPEX catchments, we do not intend to
4 propose “a model fits all approach”. It is valuable to further test, to what extent the new concept (HAND
5 is proportional to storage capacity) reflects different geomorphological and geological processes. Also the
6 assumption of HSC, to some extent, is supported by large-sample ecological field observations (Fan et al.,
7 2017), but it never means that the A_s - S_u curve of HSC can perfectly fit the other existing modules (e.g. HBV
8 and TOPMODEL). Unify all model approaches into one framework is the objective of several pioneering
9 works (e.g. Clark, et al., 2010; Fenicia et al., 2011), but out of the scope of this study. Moreover, while
10 estimating the runoff coefficient by the A_s - S_u relation, early rainfall-in the early time may cause the
11 increase of S_u/S_{uMAX} and runoff coefficient (Moore, 1985; Wang, 2018). Therefore, neglecting this influence
12 factor, the HBV module (Equation 1), TOPMODEL (Equation 2-4) and the HSC module (Equation 5-6)
13 theoretically underestimate the runoff coefficient, which needs to be further investigated.

14
15 Finally, we should not ignore the limitations of the new module's model, although it has performs better
16 performance and modelling consistency is more consistent with reality. Firstly, 1) the The threshold area
17 for the stream initiation on a stream was set as a constant value for the entire CONUS, but the variation of
18 this value in different climate, geology and landscape classes (Montgomery and Dietrich, 1989; Helmlinger
19 et al., 1993; Colombo et al., 2007; Moussa, 2008) needs to be future investigated. 2) Secondly, the The
20 discrepancy between observed and simulated saturation area needs to be further investigated, by utilizing
21 more advanced field measurements and simultaneously refining the model assumptions. To our
22 understanding, there are two four interpretations. Firstly, 1) the overestimation of the HSC model is possibly
23 possible because of the two runoff generation mechanisms – SOF and the SSF occur at the same time.
24 However, the saturated area observed by the “squishy boot” method (Ali et al., 2013), probably only
25 distinguished the areas where SOF occurs red. Subsurface stormflow, also contributes to runoff but
26 without surface runoff, cannot be observed by the “squishy boot” method. Thus, this mismatch between
27 simulation and observation probably leads to the overestimation of is saturation areas overestimation.
28 Another The second interpretation might be the different definition of “saturation”. The observed
29 saturation areas are places where 100% of soil pore volume is filled by water preferentially connected
30 to the stream network in the flat valley bottom of the BB catchment (and less related to topography, Birkel
31 et al., 2010). But the modelled saturation areas are located where soil moisture is above field capacity

1 [throughout the catchment](#), and not necessarily 100% filled with water, which probably also results in [the](#)
2 [overestimation of saturation~~ed~~ areas](#). 3) [Only the runoff generation module is calibration free, but the](#)
3 [interception and response routines ~~are still rely~~ed on calibration](#). Although we kept the interception and
4 [response routine modules the same for the four models, the variation of other calibrated parameters \(i.e.](#)
5 [\$S_{uMax}\$, \$D\$, \$K_f\$, \$K_s\$, \$T_{lagF}\$ \) may also influence model performance in both calibration and validation. 4\) \[The\]\(#\)
6 \[computational cost of the HSC and MCT is much more expensive than the two benchmark models,\]\(#\)
7 \[especially comparing with HBV, because of the calculation of \\$S_{uMax}\\$ by the MCT method, and the\]\(#\)
8 \[topographic analysis of the HSC module.\]\(#\)](#)

9 7 Summary and conclusions

10 In this study, we developed a simple [and](#), calibration-free hydrological module based on [a relative new](#)
11 [topographic index \(HAND ~~information~~\)](#), which is an excellent indicator of hydrologic similarity and a
12 physically-based index linking terrain with hydraulic gradient at the hillslope and catchment scales. We
13 assumed that the local storage capacity is closely linked to HAND. Based on this assumption and the HAND
14 spatial distribution pattern, the soil moisture (S_u) - saturated area (A_s) relation for each catchment was
15 derived, which was used to estimate the A_s of specific rainfall event based on continuous calculation of S_u .
16 Subsequently, based on the S_u - A_s relation, the HAND-based Storage Capacity curve (HSC) module was
17 developed. Then, applying the mass curve technique (MCT) approach ([Gao et al., 2014a](#)), we estimated
18 the root zone storage capacity (S_{uMax}) from observ~~able~~ hydro-climatological and vegetation data, and
19 coupled it with HSC to create the calibration-free HSC-MCT module, in which the S_{uMax} was obtained by
20 MCT, and the S_u - A_s relation was obtained by HSC. The HBV beta-function and TWI-based TOPMODEL were
21 used as two benchmark~~s~~ ~~modules~~ to test the performance of HSC and HSC-MCT on both hydrograph
22 simulation and ability to reproduce the contributing area, which was measured for different
23 hydrometeorological conditions in the Bruntland Burn catchment in Scotland. Subsequently, 323 MOPEX
24 catchments in the US were used as a large sample hydrological study to further validate the effectiveness
25 of our proposed runoff generation modules.

26 In the BB exploratory study, we found that the HSC, HBV and TOPMODEL performed comparably well to
27 reproduce the observed hydrograph. Interestingly, the S_u - A_s curves of HSC and HBV are largely comparable,
28 which illustrates the HSC curve can [likely](#) be used as a proxy for the HBV beta-function. Comparing the
29 estimated contributing area of TOPMODEL with the HSC module, we found that the results of the HSC
30 module correlate better ($R^2=0.60$) with the observed saturation~~ed~~ areas compared to TOPMODEL

1 (R²=0.50). This likely indicates that HAND maybe a better indicator to distinguish hydrological similarity
2 than TWI.

3 For the 323 MOPEX catchments, HSC improved the averaged validation value of I_{KGE} from 0.62 (HBV) and
4 0.61 (TOPMODEL) to 0.65. In 12% of the MOPEX catchments, the HSC module outperforms HBV, and in
5 not a single catchment did the calibrated HBV outperform the HSC. Comparing with TOPMODEL, the HSC
6 outperformed in 8% of the catchments, and in only 1% of catchments TOPMODEL has a better
7 performance. Not surprisingly, the I_{KGE} of HSC-MCT model was slightly reduced to 0.59, due to the non-
8 calibrated S_{uMax} , but still comparably well performed as HBV (0.62) and TOPMODEL (0.61). This illustrates
9 the robustness of both the HSC approach to derive the spatial distribution of the root zone storage
10 capacity (β) and the efficiency of the MCT method to estimate the root zone storage capacity (S_{uMax}).
11 ~~Moreover, the new module allows us to map out the saturated area, which has potential capability to be~~
12 ~~used for broader hydrological, ecological, climatological, geomorphological, and biogeochemical studies.~~

13

14 **Acknowledgement:**

15 This study was supported by National Key R&D Program of China (2017YFE0100700), [and the Key Program](#)
16 [of National Natural Science Foundation of China \(No. 41730646\)](#).

17

18 **Author contributions:**

19 H.G. and H.H.G.S. designed research; H.G. performed research; C.B., C.S., D.T and H.G. provided data,
20 among which the dynamics of the saturation areas data in the BB was provided by C.B. C.S., and D.T.; H.G.
21 analysed data; C.B. was involved in the interpretation of some of the modelling work in the BB; H.G. M.H,
22 and H.H.G.S. wrote the paper; CS and DT extensively edited the paper, and provided substantial comments
23 and constructive suggestions for scientific clarification.

24

25 **References:**

26 Anderson, M. C., Kustas, W. P., Norman, J. M., Hain, C. R., Mecikalski, J. R., Schultz, L., González-Dugo, M.
27 P., Cammalleri, C., D'Urso, G., Pimstein, A., and Gao, F.: Mapping daily evapotranspiration at field to

1 continental scales using geostationary and polar orbiting satellite imagery, *Hydrol. Earth Syst. Sci.*, 15,
2 223–239, doi:10.5194/hess-15-223-2011, 2011.

3 Andréassian V, Bourgin F, Oudin L, Mathevet T, Perrin C, Lerat J, Coron L, Berthet L. 2014. Seeking
4 genericity in the selection of parameter sets: Impact on hydrological model efficiency. *Water Resources*
5 *Research* 50 (10): 8356–8366

6 Bergström S, Forsman A. 1973. Development of a conceptual deterministic rainfall-runoff model.
7 *Hydrology Research* 4 (3): 147–170

8 Bergström S, Lindström G. 2015. Interpretation of runoff processes in hydrological modelling—experience
9 from the HBV approach. *Hydrological Processes* 29 (16): 3535–3545

10 Beven K. 2004. Robert E. Horton’s perceptual model of infiltration processes. *Hydrological Processes* 18
11 (17): 3447–3460 DOI: 10.1002/hyp.5740

12 Beven K, Freer J. 2001. A dynamic TOPMODEL. *Hydrological Processes* 15 (10): 1993–2011 DOI:
13 10.1002/hyp

14 Beven K. 1993. Prophecy, reality and uncertainty in distributed hydrological modelling. *Advances in Water*
15 *Resources* 16 (1): 41–51 DOI: [http://dx.doi.org/10.1016/0309-1708\(93\)90028-E](http://dx.doi.org/10.1016/0309-1708(93)90028-E)

16 Beven K. 1995. Linking parameters across scales: Subgrid parameterizations and scale dependent
17 hydrological models. *Hydrological Processes* 9 (September 1994): 507–525 DOI:
18 10.1002/hyp.3360090504.252

19 Beven KJ. 2012. *Rainfall–Runoff Models: The Primer*

20 Beven K., Germann P. 1982. Macropores and water-flow in soils. *Water Resour. Res.* 18, 1311–1325

21 Beven KJ, Kirkby MJ. 1979. A physically based, variable contributing area model of basin hydrology.
22 *Hydrological Sciences Bulletin* 24 (1): 43–69 DOI: 10.1080/02626667909491834

23 Beven, K., 1989. Changing ideas in hydrology – the case of physically-based models. *J. Hydrol.* 105 (1–2),
24 157–172.

25 Birkel C, Tetzlaff D, Dunn SM, Soulsby C. 2010. Towards a simple dynamic process conceptualization in
26 rainfall–runoff models using multi-criteria calibration and tracers in temperate, upland catchments.
27 *Hydrological Processes* 24 (3): 260–275

1 Birkel, C., Soulsby, C., and D. Tetzlaff (2014) Conceptual modelling to assess how the interplay of
2 hydrological connectivity, catchment storage and tracer dynamics controls non-stationary water age
3 estimates. *Hydrological Processes*, DOI: 10.1002/hyp.10414.

4 Blöschl G. 2013. Runoff prediction in ungauged basins: synthesis across processes, places and scales.
5 Cambridge University Press.

6 Budyko MI. 1971. Climate and life

7 Burt TP, McDonnell JJ. 2015. Whither field hydrology? The need for discovery science and outrageous
8 hydrological hypotheses. *Water Resources Research* 51 (8): 5919–5928 DOI: 10.1002/2014WR016839

9 Chase CG. 1992. Fluvial landsculpting and the fractal dimension of topography. *Geomorphology* 5 (1): 39–
10 57 DOI: [http://dx.doi.org/10.1016/0169-555X\(92\)90057-U](http://dx.doi.org/10.1016/0169-555X(92)90057-U)

11 Clark MP, Slater AG, Rupp DE, Woods R a., Vrugt J a., Gupta H V., Wagener T, Hay LE. 2008. Framework
12 for Understanding Structural Errors (FUSE): A modular framework to diagnose differences between
13 hydrological models. *Water Resources Research* 44: 1–14 DOI: 10.1029/2007WR006735

14 Clark, Martyn P., Dmitri Kavetski, and Fabrizio Fenicia. “Pursuing the Method of Multiple Working
15 Hypotheses for Hydrological Modeling.” *Water Resources Research* 47.9 (2011): 1–16.

16 Colombo R, Vogt J V, Soille P, Paracchini ML, de Jager A. 2007. Deriving river networks and catchments at
17 the European scale from medium resolution digital elevation data. *CATENA* 70 (3): 296–305 DOI:
18 <http://doi.org/10.1016/j.catena.2006.10.001>

19 Condon, Laura E, and Reed M Maxwell. “Evaluating the Relationship between Topography and
20 Groundwater Using Outputs from a Continental-Scale Integrated Hydrology Model.” *Water Resources*
21 *Research* 51.8 (2015): 6602–6621.

22 Duan Q, Schaake J, Andréassian V, Franks S, Goteti G, Gupta HV, Gusev YM, Habets F, Hall a., Hay L, et al.
23 2006. Model Parameter Estimation Experiment (MOPEX): An overview of science strategy and major
24 results from the second and third workshops. *Journal of Hydrology* 320 (1-2): 3–17 DOI:
25 [10.1016/j.jhydrol.2005.07.031](http://dx.doi.org/10.1016/j.jhydrol.2005.07.031)

26 Dunne T, Black RD. 1970. [Partial area contributions](http://soilandwater.bee.cornell.edu/Research/VSA/papers/DunneWRR70.pdf) to Storm Runoff in a Small New England Watershed
27 [Dense till](http://soilandwater.bee.cornell.edu/Research/VSA/papers/DunneWRR70.pdf). *Water Resources Research* 6 (5): 1296–1311 Available at:
28 <http://soilandwater.bee.cornell.edu/Research/VSA/papers/DunneWRR70.pdf>

1 Boer-Euser, T. ., H. K. McMillan, M. Hrachowitz, H. C. Winsemius, and H. H. G. Savenije (2016), Influence
2 of soil and climate on root zone storage capacity, *Water Resour. Res.*, 52, 2009–2024,
3 doi:10.1002/2015WR018115.

4 Fan, Y., Miguezmacho, G., Jobbágy, E. G., Jackson, R. B., & Oterocasal, C. (2017). Hydrologic regulation of
5 plant rooting depth. *Proceedings of the National Academy of Sciences of the United States of America*,
6 114(40), 201712381.

7 Fenicia F, Savenije HHG, Matgen P, Pfister L. 2007. A comparison of alternative multiobjective calibration
8 strategies for hydrological modeling. *Water Resources Research* 43 (3): n/a–n/a DOI:
9 10.1029/2006WR005098

10 Gao H, Hrachowitz M, Schymanski SJ, Fenicia F, Sriwongsitanon N, Savenije HHG. 2014a. Climate controls
11 how ecosystems size the root zone storage capacity at catchment scale. *Geophysical Research Letters* 41
12 (22): 7916–7923 DOI: 10.1002/2014gl061668

13 Gao H, Hrachowitz M, Fenicia F, Gharari S, Savenije HHG. 2014b. Testing the realism of a topography-
14 driven model (FLEX-Topo) in the nested catchments of the Upper Heihe, China. *Hydrology and Earth*
15 *System Sciences* 18 (5): 1895–1915 DOI: 10.5194/hess-18-1895-2014

16 Gao H, Hrachowitz M, Sriwongsitanon N, Fenicia F, Gharari S, Savenije HHG. 2016. Accounting for the
17 influence of vegetation and landscape improves model transferability in a tropical savannah region. *Water*
18 *Resources Research* 52 (10): 7999–8022 DOI: 10.1002/2016WR019574

19 Gao H, Cai H, Zheng D. 2017. Understand the impacts of landscape features on the shape of storage
20 capacity curve and its influence on flood. *Hydrology Research*. DOI: Hydrology-D-16-00245R3

21 Gao J, Holden J, Kirkby M. 2016. The impact of land-cover change on flood peaks in peatland basins. *Water*
22 *Resources Research* 52 (5): 3477–3492 DOI: 10.1002/2015WR017667

23 Gharari S, Hrachowitz M, Fenicia F, Savenije HHG. 2011. Hydrological landscape classification:
24 investigating the performance of HAND based landscape classifications in a central European meso-scale
25 catchment. *Hydrology and Earth System Sciences* 15 (11): 3275–3291 DOI: 10.5194/hess-15-3275-2011

26 Gharari S, Hrachowitz M, Fenicia F, Gao H, Savenije HHG. 2014. Using expert knowledge to increase
27 realism in environmental system models can dramatically reduce the need for calibration. *Hydrology and*
28 *Earth System Sciences* 18 (12): 4839–4859 DOI: 10.5194/hess-18-4839-2014

1 Gharari, S. On the role of model structure in hydrological modeling: Understanding models, PhD
2 dissertation, 2016

3 Gomes GJC, Vrugt JA, Vargas EA. 2016. Toward improved prediction of the bedrock depth underneath
4 hillslopes: Bayesian inference of the bottom-up control hypothesis using high-resolution topographic data.
5 *Water Resources Research* 52 (4): 3085–3112 DOI: 10.1002/2015WR018147

6 Grabs T, Seibert J, Bishop K, Laudon H. 2009. Modeling spatial patterns of saturated areas: A comparison
7 of the topographic wetness index and a dynamic distributed model. *Journal of Hydrology* 373 (1): 15–23

8 De Groen MM, Savenije HHG. 2006. A monthly interception equation based on the statistical
9 characteristics of daily rainfall. *Water Resources Research* 42 (12): n/a–n/a DOI: 10.1029/2006WR005013

10 Gumbel, E. J. (1935), Les valeurs extrêmes des distributions statistiques, *Annales de l'institut Henri*
11 *Poincaré*, 5(2), 115–158.

12 Gupta H V., Kling H, Yilmaz KK, Martinez GF. 2009. Decomposition of the mean squared error and NSE
13 performance criteria: Implications for improving hydrological modelling. *Journal of Hydrology* 377 (1-2):
14 80–91 DOI: 10.1016/j.jhydrol.2009.08.003

15 Hargreaves GH, Samani ZA. 1985. Reference crop evapotranspiration from temperature. *Applied*
16 *engineering in agriculture* 1 (2): 96–99

17 Haria AH, Shand P. 2004. Evidence for deep sub-surface flow routing in forested upland Wales:
18 implications for contaminant transport and stream flow generation. *Hydrology and Earth System Sciences*
19 *Discussions* 8 (3): 334–344

20 Harte J. 2002. Toward a synthesis of the Newtonian and Darwinian worldviews. *Physics Today* 55 (10): 29–
21 34 DOI: 10.1063/1.1522164

22 Helmlinger KR, Kumar P, Foufoula-Georgiou E. 1993. On the use of digital elevation model data for
23 Hortonian and fractal analyses of channel network. *Water Resources Research* 29: 2599–2613.

24 Hewlett JD. 1961. Soil moisture as a source of base flow from steep mountain watersheds. Southeastern
25 Forest Experiment Station, US Department of Agriculture, Forest Service.

26 Hewlett JD, Troendle CA. 1975. Non point and diffused water sources: a variable source area problem. In
27 *Watershed Management; Proceedings of a Symposium*.

1 Hooshyar M, Wang D, Kim S, Medeiros SC, Hagen SC. 2016. Valley and channel networks extraction based
2 on local topographic curvature and k-means clustering of contours. *Water Resources Research* 52 (10):
3 8081–8102

4 Horton, R.E., 1933. The role of infiltration in the hydrologic cycle. *Trans. Am. Geophys. Union* 14, 446–460.

5 Hrachowitz M, Savenije HHG, Blöschl G, McDonnell JJ, Sivapalan M, Pomeroy JW, Arheimer B, Blume T,
6 Clark MP, Ehret U, et al. 2013. A decade of Predictions in Ungauged Basins (PUB)—a review. *Hydrological
7 Sciences Journal* 58 (6): 1198–1255 DOI: 10.1080/02626667.2013.803183

8 Hu, G. and Jia, L.: Monitoring of evapotranspiration in a semiarid inland river basin by combining
9 microwave and optical remote sensing observations, *Remote Sens.*, 7, 3056–3087,
10 doi:10.3390/rs70303056, 2015.

11 Iorgulescu I, Jordan J-P. 1994. Validation of TOPMODEL on a small Swiss catchment. *Journal of Hydrology*
12 159 (1): 255–273 DOI: [http://dx.doi.org/10.1016/0022-1694\(94\)90260-7](http://dx.doi.org/10.1016/0022-1694(94)90260-7)

13 ~~[Jenson SK, Domingue JO. 1988. Extracting topographic structure from digital elevation data for geographic
14 information system analysis. *Photogrammetric engineering and remote sensing* 54 \(11\): 1593–1600](#)~~

15 Kirchner JW. 2006. Getting the right answers for the right reasons: Linking measurements, analyses, and
16 models to advance the science of hydrology. *Water Resources Research* 42 (3): n/a–n/a DOI:
17 10.1029/2005WR004362

18 Kleidon A, Lorenz RD. 2004. *Non-equilibrium thermodynamics and the production of entropy: life, earth,
19 and beyond.* Springer Science & Business Media.

20 ~~[Kollat, J. B., P. M. Reed, and T. Wagener. "When are multiobjective calibration trade - offs in hydrologic
21 models meaningful?." *Water Resources Research* 48.3\(2012\):3520.](#)~~

22 Liang X, Lettenmaier DP, Wood EF, Burges SJ. 1994. A simple hydrologically based model of land surface
23 water and energy fluxes for general circulation models. *Journal of Geophysical Research* 99 (D7): 14415
24 DOI: 10.1029/94JD00483

25 Liu D, Tian F, Hu H, Hu H. 2012. The role of run-on for overland flow and the characteristics of runoff
26 generation in the Loess Plateau, China. *Hydrological Sciences Journal* 57 (6): 1107–1117 DOI:
27 10.1080/02626667.2012.695870

- 1 Maxwell, Reed M, and Laura E Condon. "Connections between Groundwater Flow and Transpiration
2 Partitioning." *Science* 353.6297 (2016): 377 LP – 380.
- 3 McDonnell JJ, Sivapalan M, Vaché K, Dunn S, Grant G, Haggerty R, Hinz C, Hooper R, Kirchner J, Roderick
4 ML, et al. 2007. Moving beyond heterogeneity and process complexity: A new vision for watershed
5 hydrology. *Water Resources Research* 43 (7): n/a–n/a DOI: 10.1029/2006WR005467
- 6 McDonnell JJ. 2013. Are all runoff processes the same? *Hydrological Processes* 27 (26): 4103–4111 DOI:
7 10.1002/hyp.10076
- 8 Merz R, Blöschl G. 2004. Regionalisation of catchment model parameters. *Journal of Hydrology* 287 (1-4):
9 95–123 DOI: 10.1016/j.jhydrol.2003.09.028
- 10 Milly, P. C. D. (1994), Climate, soil water storage, and the average annual water balance, *Water Resour.*
11 *Res.*, 30(7), 2143–2156.
- 12 Molenat J, Gascuel-Oudou C, Ruiz L, Gruau G. 2008. Role of water table dynamics on stream nitrate export
13 and concentration in agricultural headwater catchment (France). *Journal of Hydrology* 348 (3): 363–378
- 14 Molénat J, Gascuel-Oudou C, Davy P, Durand P. 2005. How to model shallow water-table depth variations:
15 the case of the Kervidy-Naizin catchment, France. *Hydrological Processes* 19 (4): 901–920
- 16 Montgomery DR, Dietrich WE. 1989. Source areas, drainage density, and channel initiation. *Water*
17 *Resources Research* 25 (8): 1907–1918
- 18 [Moore, R. J. \(1985\), The probability-distributed principle and runoff production at point and basin scales,](#)
19 [Hydrol. Sci. J., 30, 273-297.](#)
- 20 Moussa R. 2008. Effect of channel network topology, basin segmentation and rainfall spatial distribution
21 on the geomorphologic instantaneous unit hydrograph transfer function. *Hydrological Processes* 22 (3):
22 395–419 DOI: 10.1002/hyp.6612
- 23 Moussa R. 2009. Definition of new equivalent indices of Horton-Strahler ratios for the derivation of the
24 Geomorphological Instantaneous Unit Hydrograph. *Water Resources Research* 45 (9): n/a–n/a DOI:
25 10.1029/2008WR007330
- 26 ~~[Neuweiler I, Helmig R. Debates—Hypothesis testing in hydrology: A subsurface perspective. *Water*](#)~~
27 ~~[Resources Research: n/a–n/a DOI: 10.1002/2016WR020047](#)~~

1 Nobre a. D, Cuartas L a., Hodnett M, Rennó CD, Rodrigues G, Silveira a., Waterloo M, Saleska S. 2011.
2 Height Above the Nearest Drainage - a hydrologically relevant new terrain model. Journal of Hydrology
3 404 (1-2): 13–29 DOI: 10.1016/j.jhydrol.2011.03.051

4 ~~O’Callaghan JF, Mark DM. 1984. The extraction of drainage networks from digital elevation data.
5 Computer vision, graphics, and image processing 28 (3): 323–344~~

6 Orth R, Staudinger M, Seneviratne SI, Seibert J, Zappa M. 2015. Does model performance improve with
7 complexity? A case study with three hydrological models. Journal of Hydrology 523: 147–159 DOI:
8 <http://doi.org/10.1016/j.jhydrol.2015.01.044>

9 Passalacqua P, Belmont P, Staley DM, Simley JD, Arrowsmith JR, Bode CA, Crosby C, DeLong SB, Glenn NF,
10 Kelly SA, et al. 2015. Analyzing high resolution topography for advancing the understanding of mass and
11 energy transfer through landscapes: A review. Earth-Science Reviews 148: 174–193 DOI:
12 <http://doi.org/10.1016/j.earscirev.2015.05.012>

13 Pelletier JD, Barron-Gafford GA, Breshears DD, Brooks PD, Chorover J, Durcik M, Harman CJ, Huxman TE,
14 Lohse KA, Lybrand R, et al. 2013. Coevolution of nonlinear trends in vegetation, soils, and topography with
15 elevation and slope aspect: A case study in the sky islands of southern Arizona. Journal of Geophysical
16 Research: Earth Surface 118 (2): 741–758 DOI: 10.1002/jgrf.20046

17 Perrin C, Michel C, Andréassian V. 2001. Does a large number of parameters enhance model performance?
18 Comparative assessment of common catchment model structures on 429 catchments. Journal of
19 Hydrology 242 (3-4): 275–301 DOI: 10.1016/S0022-1694(00)00393-0

20 Ponce, V. M., and R. H. Hawkins (1996), Runoff curve number: Has it reached maturity?, J. Hydrol. Eng.,
21 1(1), 11–19.

22 Rempe, D. M., and W. E. Dietrich (2014), A bottom-up control on fresh-bedrock topography under
23 landscapes, Proc. Natl. Acad. Sci. U. S. A., 111(18), 6576–6581, doi:10.1073/pnas.1404763111.

24 Rennó, C.D., Nobre, A.D., Cuartas, L.A., Soares, J.V., Hodnett, M.G., Tomasella, J., Waterloo, M., 2008.
25 HAND, a new terrain descriptor using SRTM-DEM; mapping terra-firme rainforest environments in
26 Amazonia. Remote Sensing of Environment 112, 3469–3481.

27 Rodriguez-Iturbe, I., and A. Rinaldo, Fractal River Basins: Chance and Self-Organization, Cambridge Univ.
28 Press, 547 pp., New York, 1997.

1 Samaniego L, Kumar R, Attinger S. 2010. Multiscale parameter regionalization of a grid-based hydrologic
2 model at the mesoscale. *Water Resources Research* 46 (5): n/a–n/a DOI: 10.1029/2008WR007327

3 ~~Savenije HHG. 2009. HESS Opinions ‘The art of hydrology’. *Hydrology and Earth System Sciences* 13 (2):~~
4 ~~157–161 DOI: 10.5194/hess-13-157-2009~~

5 Savenije, H. H. G.: HESS Opinions “Topography driven conceptual modelling (FLEX-Topo)”, *Hydrol. Earth*
6 *Syst. Sci.*, 14, 2681–2692, doi:10.5194/hess-14-2681-2010, 2010.

7 Savenije HHG, Hrachowitz M. 2017. HESS Opinions ‘Catchments as meta-organisms – a new blueprint for
8 hydrological modelling’. *Hydrol. Earth Syst. Sci.* 21 (2): 1107–1116 DOI: 10.5194/hess-21-1107-2017

9 Schaake, J., S. Cong, and Q. Duan (2006), *The US MOPEX data set*, IAHS Publ., 307, 9.

10 Seibert J, Stendahl J, Sørensen R. 2007. Topographical influences on soil properties in boreal forests.
11 *Geoderma* 141 (1-2): 139–148 DOI: 10.1016/j.geoderma.2007.05.013

12 Shand P, Haria AH, Neal C, Griffiths K, Goody D, Dixon AJ, Hill T, Buckley DK, Cunningham J. 2005.
13 Hydrochemical heterogeneity in an upland catchment: further characterisation of the spatial, temporal
14 and depth variations in soils, streams and groundwaters of the Plynlimon forested catchment, Wales.
15 *Hydrology and Earth System Sciences* 9 (6): 621–644

16 Sørensen R, Seibert J. 2007. Effects of DEM resolution on the calculation of topographical indices: TWI and
17 its components. *Journal of Hydrology* 347 (1): 79–89 DOI:
18 <http://dx.doi.org/10.1016/j.jhydrol.2007.09.001>

19 Sivapalan M, Woods RA, Kalma JD. 1997. Variable bucket representation of TOPMODEL and investigation
20 of the effects of rainfall heterogeneity. *Hydrological processes* 11 (9): 1307–1330

21 Sivapalan M, Takeuchi K, Franks SW, Gupta VK, Karambiri H, Lakshmi V, Liang X, McDonnell JJ, Mendiondo
22 EM, O’Connell PE, et al. 2003. IAHS Decade on Predictions in Ungauged Basins (PUB), 2003–2012: Shaping
23 an exciting future for the hydrological sciences. *Hydrological Sciences Journal* 48 (6): 857–880 DOI:
24 10.1623/hysj.48.6.857.51421

25 Sivapalan M. 2009. The secret to ‘doing better hydrological science’: change the question! *Hydrological*
26 *Processes* 23 (9): 1391–1396 DOI: 10.1002/hyp.7242

27 Sivapalan M, Blöschl G. 2015. Time scale interactions and the coevolution of humans and water. *Water*
28 *Resources Research* 51 (9): 6988–7022 DOI: 10.1002/2015WR017896

1 Soulsby C., Birkel C., Geris J., Dick J., Tunaley, C. and Tetzlaff, D. (2015) Stream water age distributions
2 controlled by storage dynamics and non-linear hydrologic connectivity: modelling with high resolution
3 isotope data. *Water Resources Research*. DOI: 10.1002/2015WR017888

4 Soulsby C, Bradford J, Dick J, McNamara JP, Geris J, Lessels J, Blumstock M, Tetzlaff D. 2016. Using
5 geophysical surveys to test tracer-based storage estimates in headwater catchments. *Hydrological
6 Processes* 30 (23): 4434–4445 DOI: 10.1002/hyp.10889

7 Sklash MG, Farvolden RN. 1979. The role of groundwater in storm runoff. *Journal of Hydrology* 43 (1): 45–
8 65 DOI: [http://dx.doi.org/10.1016/0022-1694\(79\)90164-1](http://dx.doi.org/10.1016/0022-1694(79)90164-1)

9 Tetzlaff, D., Birkel, C., Dick, J., and C. Soulsby (2014) Storage dynamics in hydrogeological units control
10 hillslope connectivity, runoff generation and the evolution of catchment transit time distributions. *Water
11 Resources Research*, DOI: 10.1002/2013WR014147.

12 Troch P a., Carrillo G, Sivapalan M, Wagener T, Sawicz K. 2013. Climate-vegetation-soil interactions and
13 long-term hydrologic partitioning: signatures of catchment co-evolution. *Hydrology and Earth System
14 Sciences* 17 (6): 2209–2217 DOI: 10.5194/hess-17-2209-2013

15 Van Beek, L.P.H. and M.F.P. Bierkens (2008), *The Global Hydrological Model PCR-GLOBWB:
16 Conceptualization, Parameterization and Verification*, Report Department of Physical Geography, Utrecht
17 University, Utrecht, The Netherlands, <http://vanbeek.geo.uu.nl/suppinfo/vanbeekbierkens2009.pdf>

18 Vrugt J a. 2003. Effective and efficient algorithm for multiobjective optimization of hydrologic models.
19 *Water Resources Research* 39 (8): 1–19 DOI: 10.1029/2002WR001746

20 Wang D, Tang Y. 2014. A one-parameter Budyko model for water balance captures emergent behavior in
21 darwinian hydrologic models. *Geophysical Research Letters* 41 (13): 4569–4577

22 [Wang, D.: A new probability density function for spatial distribution of soil water storage capacity leads
23 to SCS curve number method, *Hydrol. Earth Syst. Sci. Discuss.*, <https://doi.org/10.5194/hess-2018-32>, in
24 \[review, 2018.\]\(#\)](#)

25 Wang-Erlandsson L, Bastiaanssen WGM, Gao H, Jägermeyr J, Senay GB, van Dijk AIJM, Guerschman JP,
26 Keys PW, Gordon LJ, Savenije HHG. 2016. Global root zone storage capacity from satellite-based
27 evaporation. *Hydrol. Earth Syst. Sci.* 20 (4): 1459–1481 DOI: 10.5194/hess-20-1459-2016

28 Weiler M., McDonnell J. J. 2007 Conceptualizing lateral preferential flow and flow networks and simulating
29 the effects on gauged and ungauged hillslopes. *Water Resour. Res.* 43, W03403

1 Ye A, Duan Q, Yuan X, Wood EF, Schaake J. 2014. Hydrologic post-processing of MOPEX streamflow
2 simulations. *Journal of Hydrology* 508: 147–156 DOI: 10.1016/j.jhydrol.2013.10.055

3 Zehe E., Fluehler H. 2001. Preferential transport of Isoproturon at a plot scale and a field scale tile-drained
4 site. *J. Hydrol.* 247, 100–115

5 Zehe E, Ehret U, Blume T, Kleidon A, Scherer U, Westhoff M. 2013. A thermodynamic approach to link self-
6 organization, preferential flow and rainfall-runoff behaviour. *Hydrol. Earth Syst. Sci.* 17 (11): 4297–4322
7 DOI: 10.5194/hess-17-4297-2013

8 Zhao R-J, Zuang Y, Fang L, Liu X, Zhang Q. 1980. The Xinanjiang model. *Hydrological forecasting —*
9 *Prévisions hydrologiques* 1980 (129): 351–356

10

11

12 Table 1. The parameters of the models, and their prior ranges for calibration. (* S_{uMax} is a parameter in HBV,
13 TOPMODEL and the HSC model, but HSC-MCT model does not have S_{uMax} as a free parameter; ** β is a parameter in
14 HBV model, but not in TOPMODEL, HSC and HSC-MCT models)

Parameter	Explanation	Prior range for calibration
S_{iMax} (mm)	Maximum interception capacity	2
S_{uMax} (mm)*	The root zone storage capacity	(10, 1000)
β (-)**	The shape of the storage capacity curve	(0.01, 5)
C_e (-)	Soil moisture threshold for reduction of evaporation	(0.1, 1)
D (-)	Splitter to fast and slow response reservoirs	(0, 1)
T_{lagF} (d)	Lag time from rainfall to peak flow	(0, 10)
K_f (d)	The fast recession coefficient	(1, 20)
K_s (d)	The slow recession coefficient	(20, 400)

15

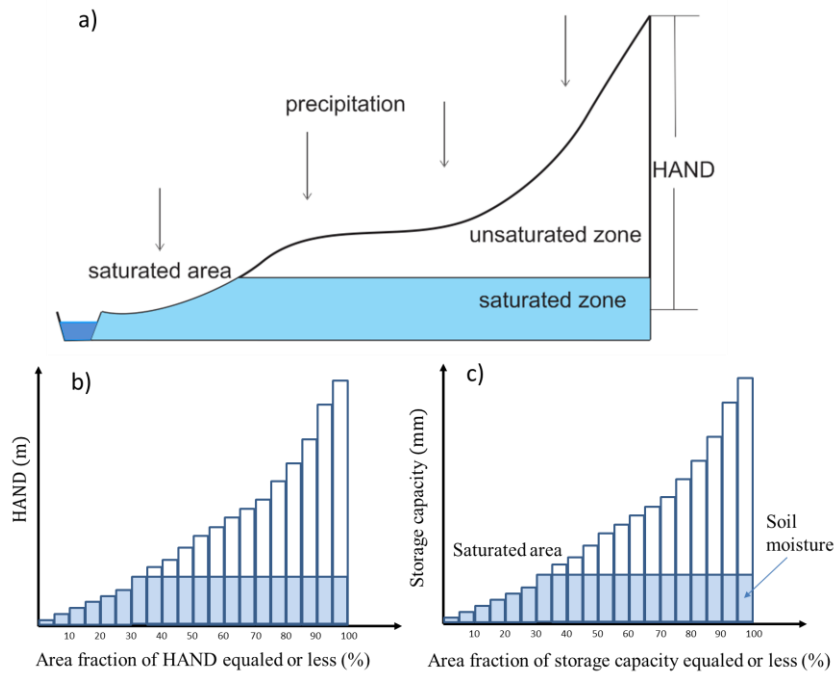
16

17 Table 2. The water balance and constitutive equations used in models. (Function (15)* is used in the HBV model, but
18 not used in the TOPMODEL, HSC and HSC-MCT models)

reservoirs	Water balance equations	Constitutive equations
Interception reservoir	$\frac{dS_i}{dt} = P - E_i - P_e \quad (8)$	$E_i = \begin{cases} E_p; S_i > 0 \\ 0; S_i = 0 \end{cases} \quad (9)$ $P_e = \begin{cases} 0; S_i < S_{iMax} \\ P; S_i = S_{iMax} \end{cases} \quad (10)$
Unsaturated reservoir	$\frac{dS_u}{dt} = P_e - E_a - R_u \quad (11)$	$\frac{R_u}{P_e} = \left(\frac{S_u}{S_{uMax}} \right)^\beta \quad (12)^*$ $\frac{E_a}{E_p - E_i} = \frac{S_u}{C_e S_{uMax}} \quad (13)$
Splitter and Lag function		$R_f = R_u D \quad (17); R_s = R_u (1 - D) \quad (14)$ $R_{fl}(t) = \sum_{i=1}^{T_{lagf}} c_f(i) \cdot R_f(t - i + 1) \quad (15)$ $c_f(i) = i / \sum_{u=1}^{T_{lagf}} u \quad (16)$
Fast reservoir	$\frac{dS_f}{dt} = R_f - Q_f \quad (17)$	$Q_f = S_f / K_f \quad (18)$
Slow reservoir	$\frac{dS_s}{dt} = R_s - Q_s \quad (19)$	$Q_s = S_s / K_s \quad (20)$

1

2

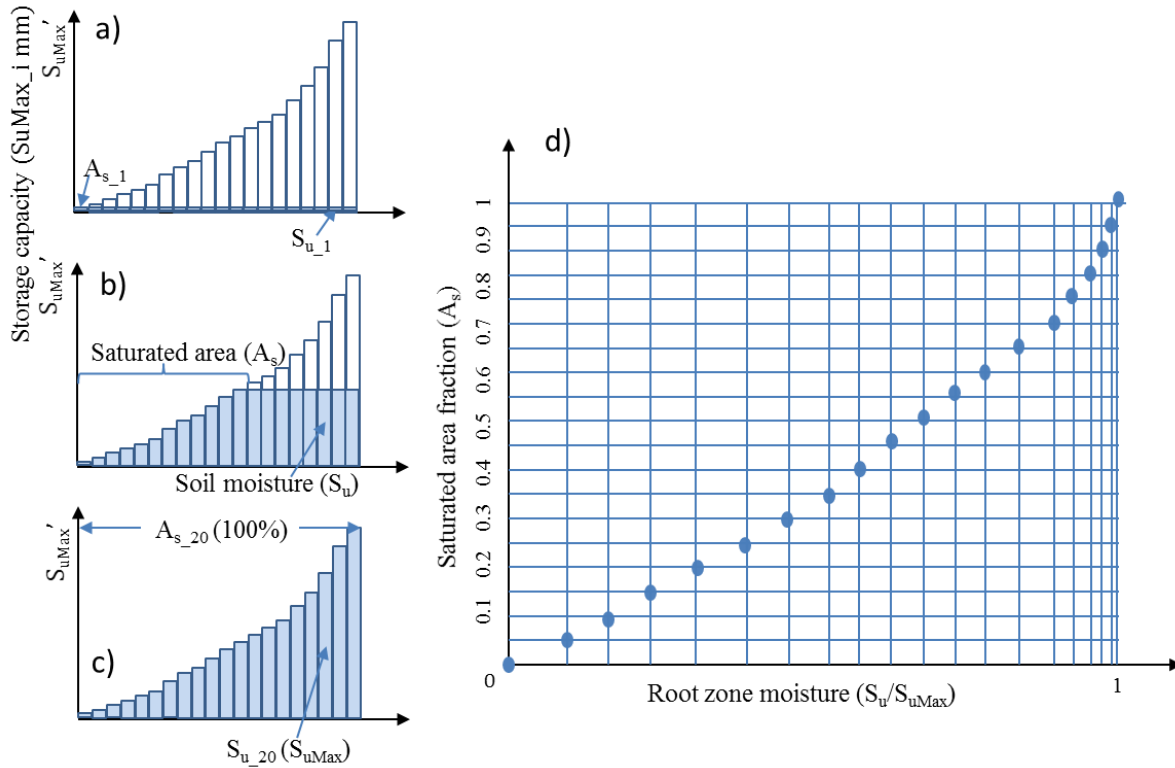


1

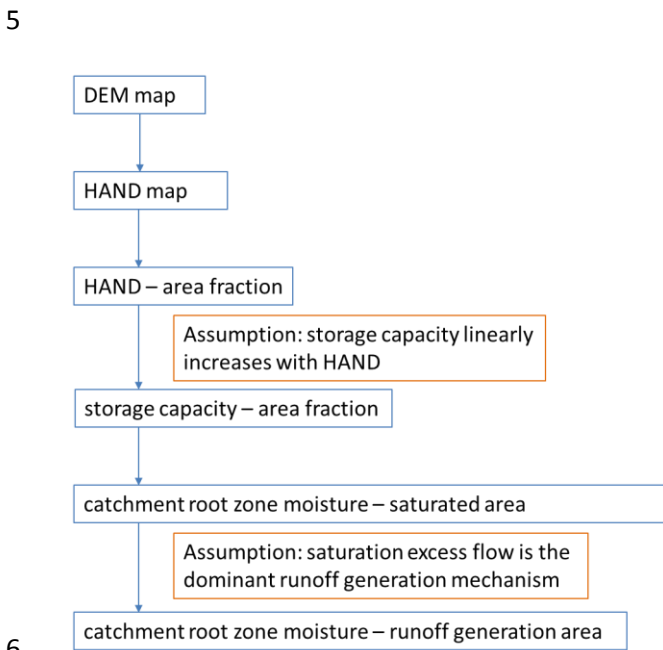
2 Figure 1. The perceptual model of the HAND-based Storage Capacity curve (HSC) model. a) shows the representative
 3 hillslope profile in nature, and the saturated area, unsaturated zone and saturated zone; b) shows the relationship
 4 between HAND bands and their corresponded area fraction; c) shows the relationship between storage capacity-
 5 area fraction-soil moisture-saturated area, based on the assumption that storage capacity linearly increases with
 6 HAND values.

7

8

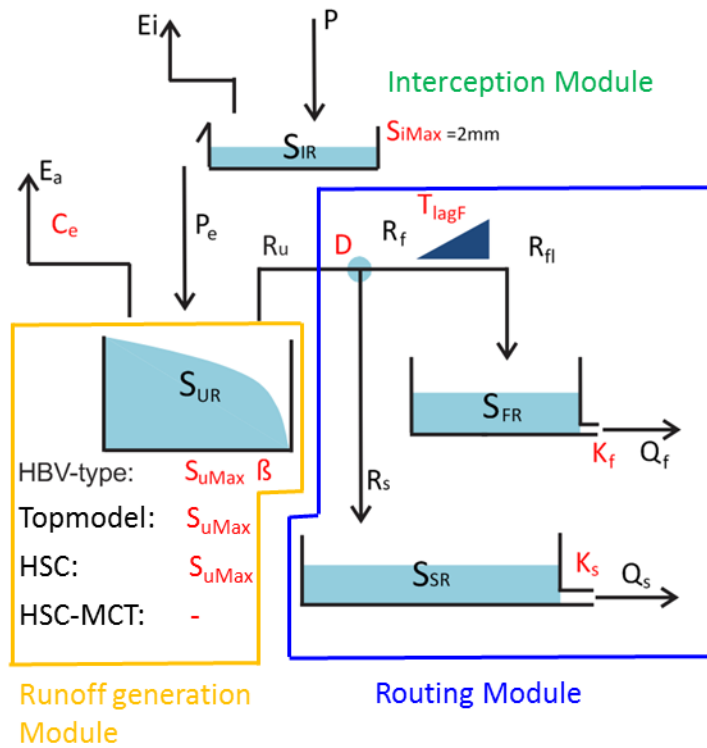


1
 2 Figure 2. The conceptual model of the HSC model. a), b) and c) illustrate the relationship between soil moisture (S_u)
 3 and saturated area (A_s) in different soil moisture conditions. In d), 20 different S_u - A_s conditions are plotted, which
 4 allow us to estimate A_s from S_u .



6
 7 Figure 3. The procedures estimating runoff generation by the HSC model and its two hypotheses.

1

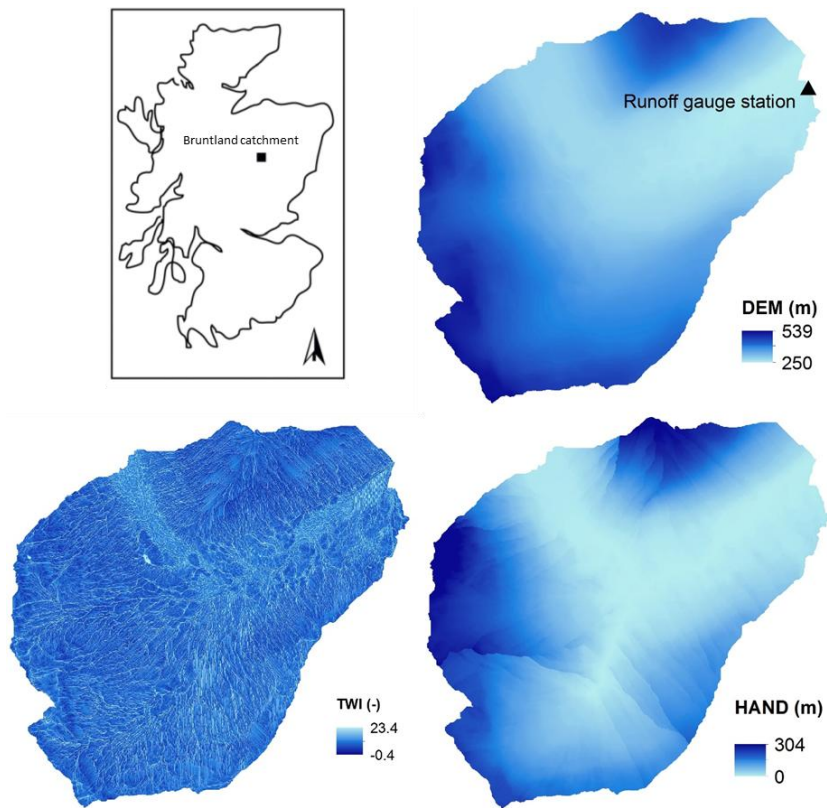


2

3 Figure 4. Model structure and free parameters, involving four runoff generation models (HBV-type, TOPMODEL, HSC,
4 and HSC -MCT). HBV-type has S_{uMax} and beta two free parameters; TOPMODEL and HSC models have S_{uMax} as one
5 free parameter; and HSC-MCT model does not have free parameter. In order to simplify calibration process and
6 make fair comparison, the interception storage capacity (S_{iMax}) was fixed as 2mm.

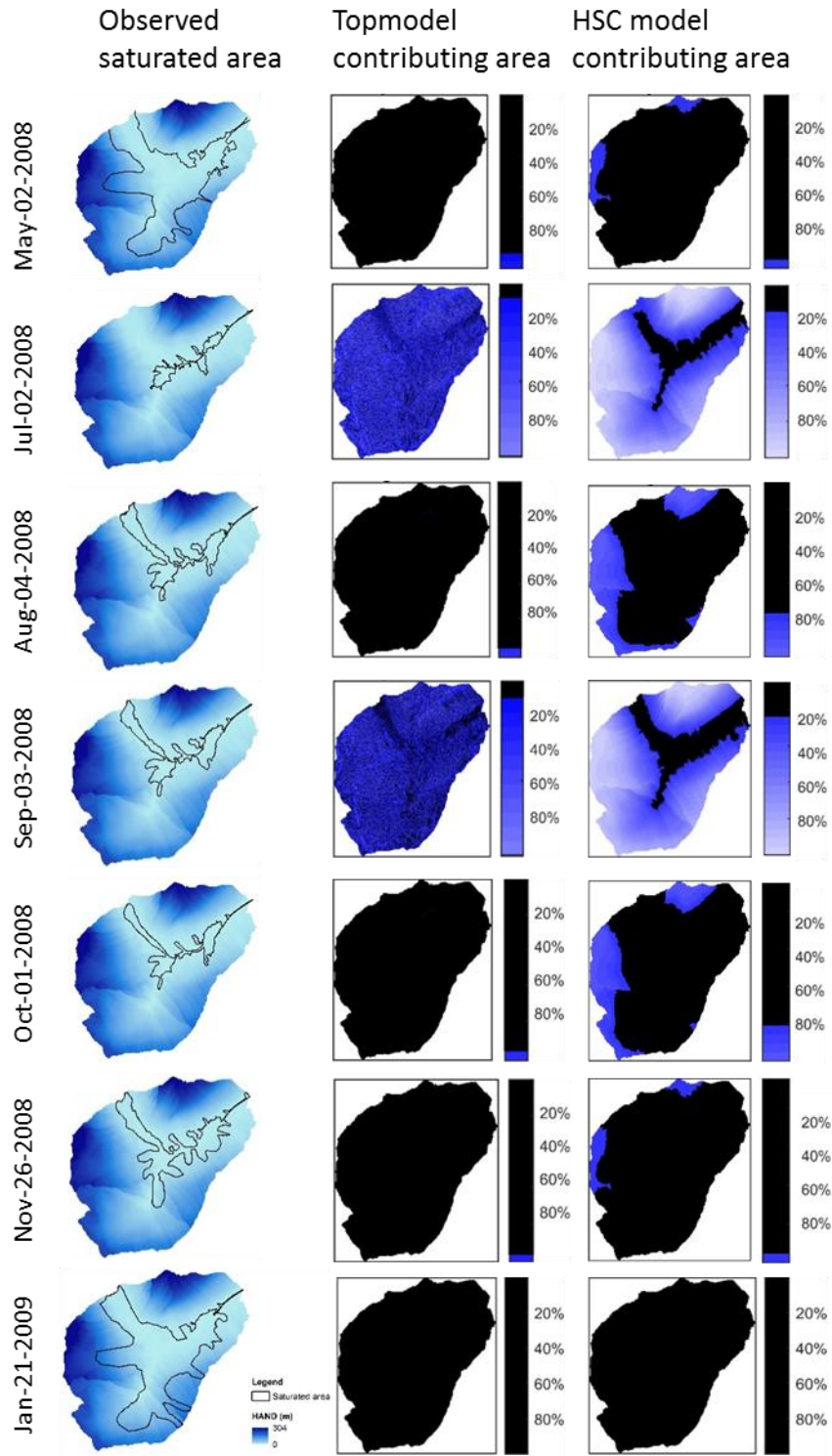
7

8

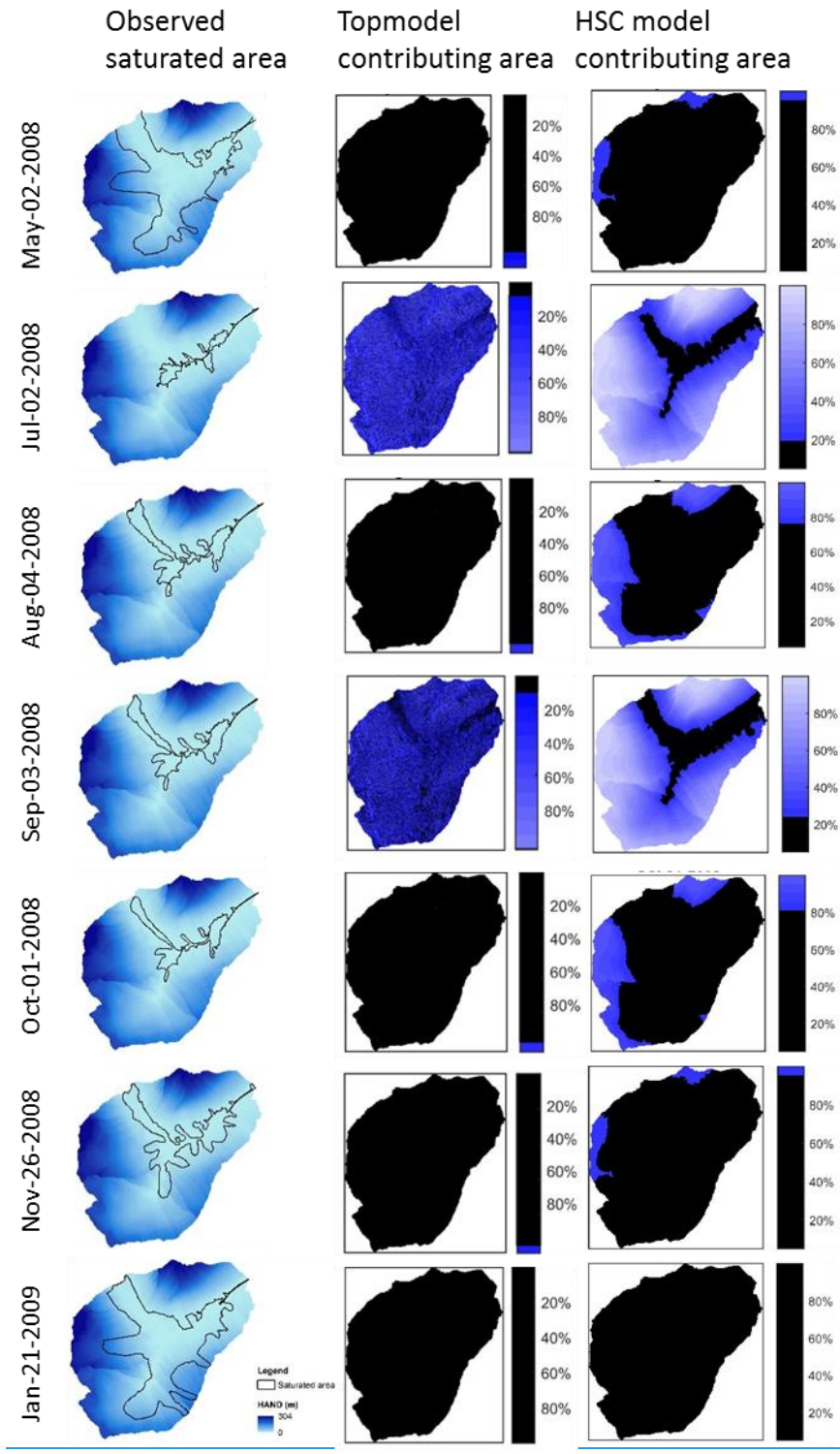


1
 2 Figure 5. (a) Study site location of the Bruntland Burn catchment within Scotland; (b) digital elevation model (DEM)
 3 of the Bruntland Burn catchment; (c) the topographic wetness index map of the Bruntland Burn catchment; (d) the
 4 height above the nearest drainage (HAND) map of the Bruntland Burn catchment.

5

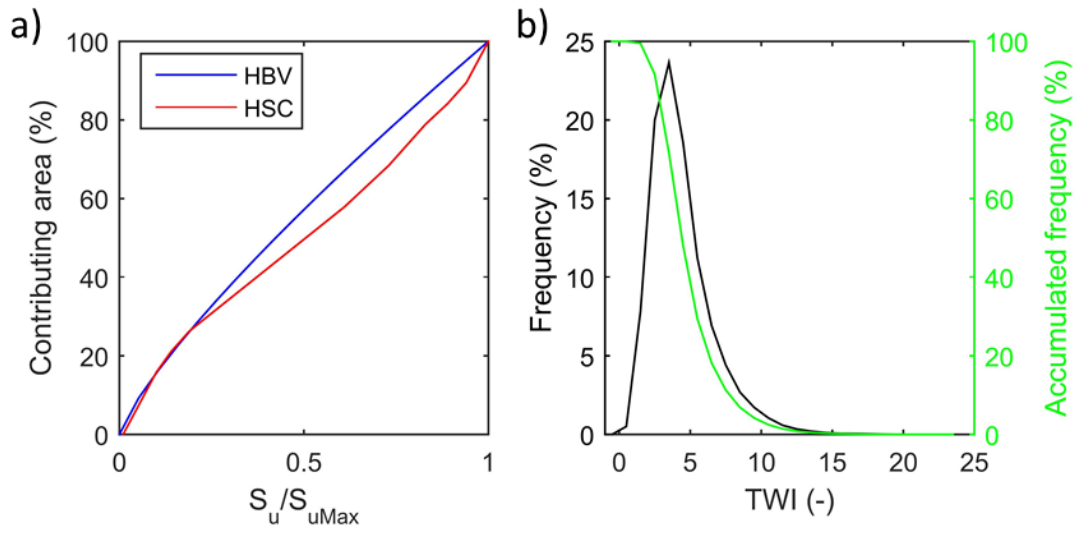


1

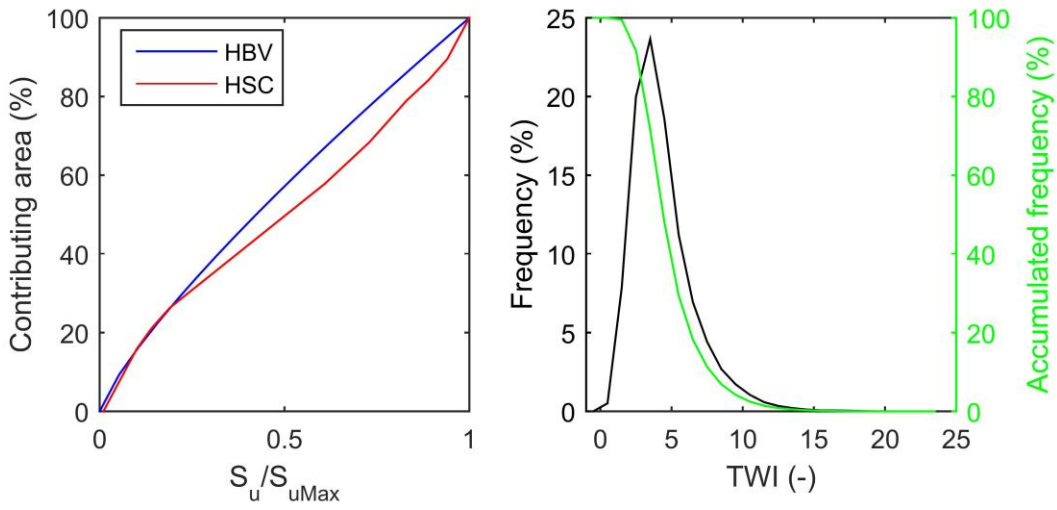


1
2
3
4

Figure 6. The measured saturated areas and the simulated contributing areas by TOPMODEL and HSC models.



1

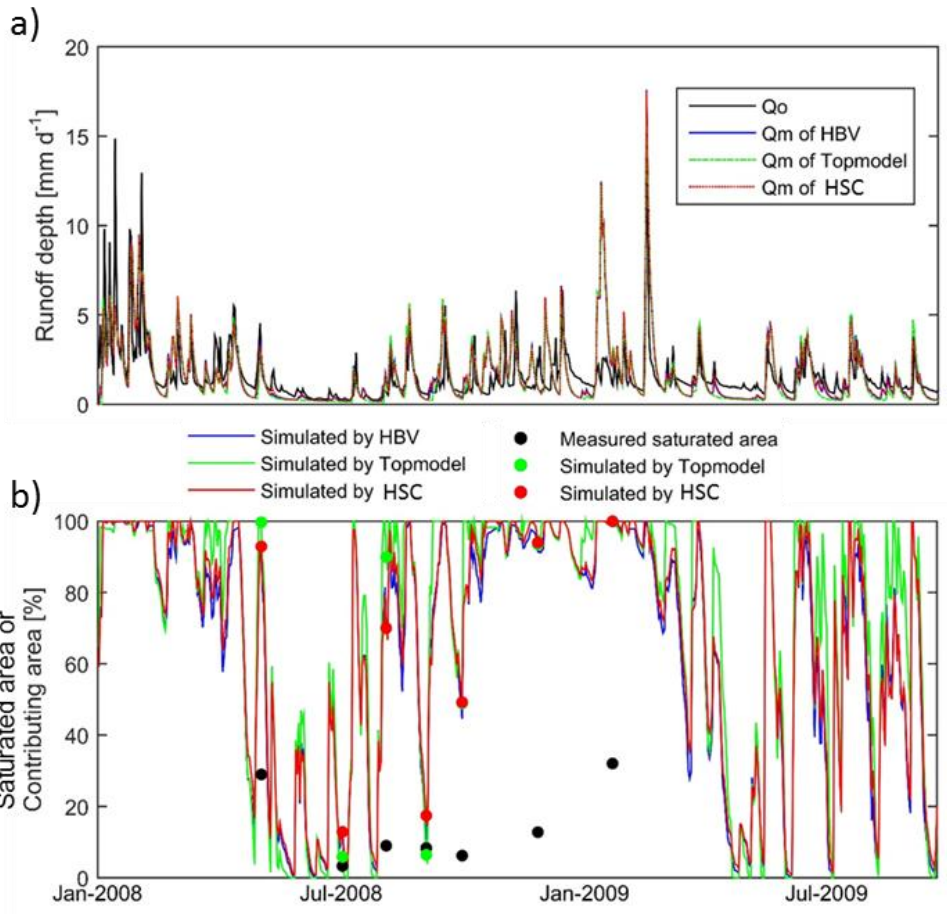


2

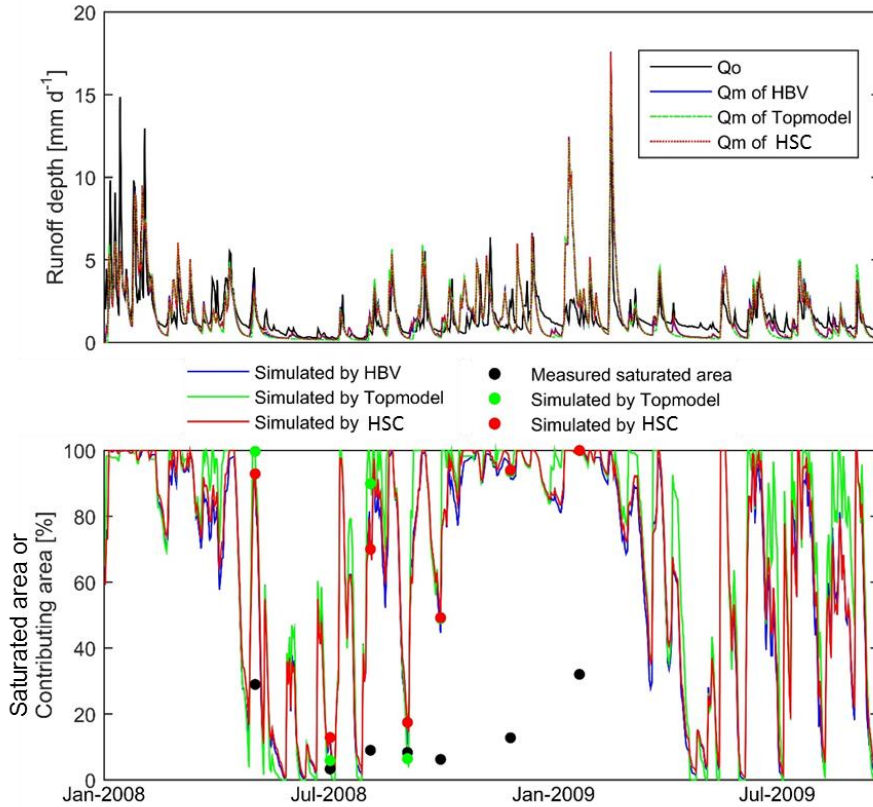
3 Figure 7. The curves of the beta function of HBV model, and the S_u - A_s curve generated by HSC model (the left figure).

4 The frequency and accumulated frequency of the TWI in the Bruntland Burn catchment (the right figure).

5

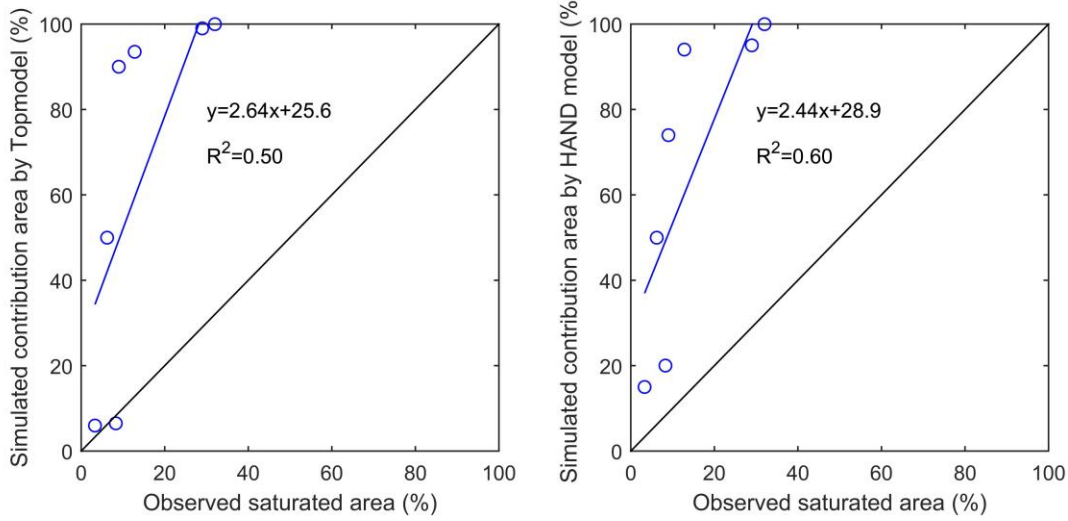
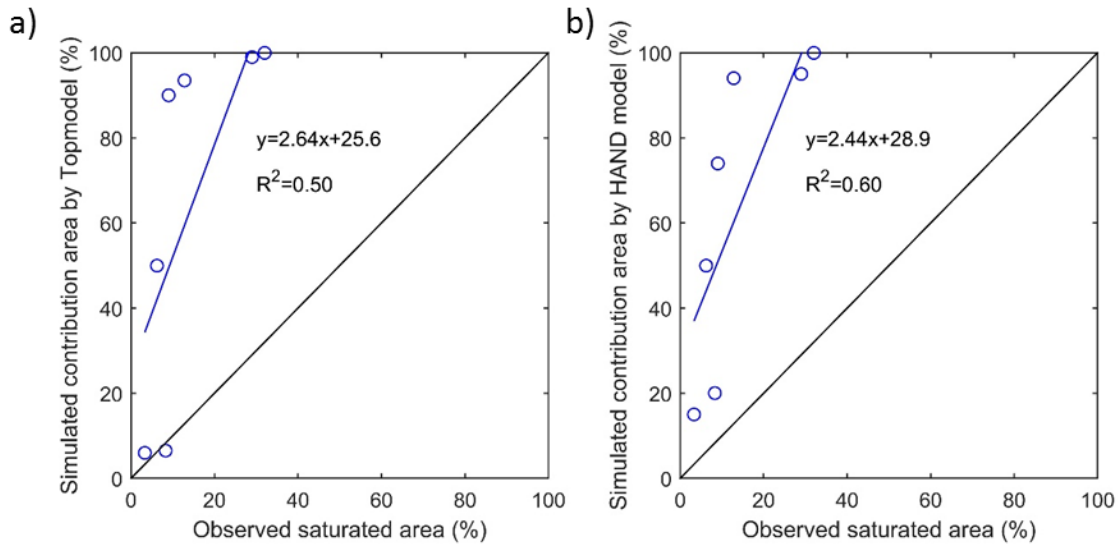


1



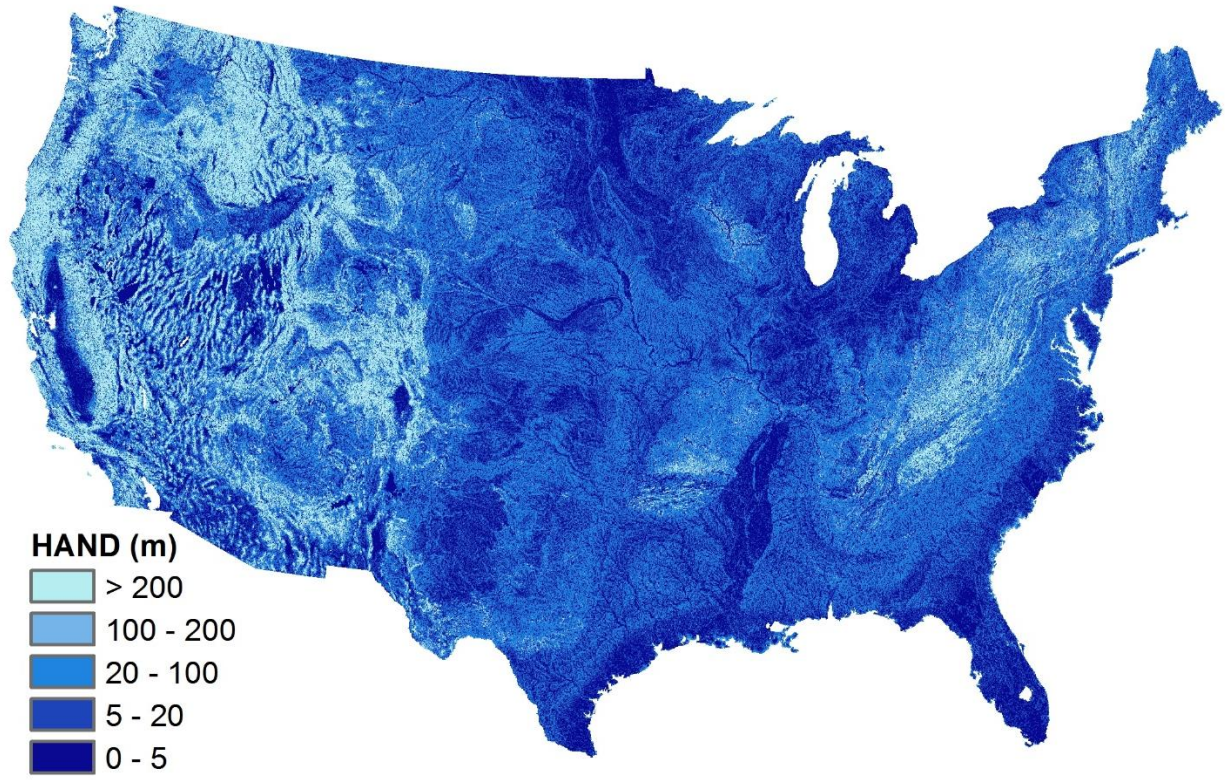
1
2
3
4
5
6
7
8
9

Figure 8. a) The observed hydrograph (Qo, black line) of the Bruntland Burn catchment in 2008. And the simulated hydrographs (Qm) by HBV model (blue line), TOPMODEL (green dash line), HSC model (red dash line); b) ~~And the comparison of the observed saturated area of 7 days (black dots) and simulated relative soil moistures, i.e. HBV (blue line), TOPMODEL (green line and dots), HSC (red line and dots).~~ ~~And the observed saturated area of 7 days (black dots), and the correspondent simulated contributing area by TOPMODEL (green dots) and by HSC model (red dots).~~



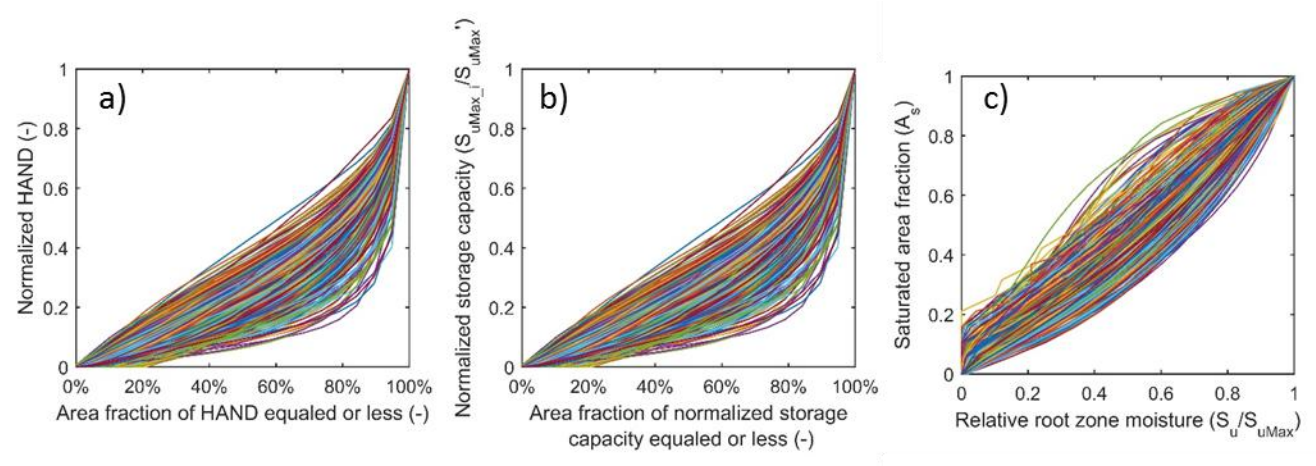
3 Figure 9. The comparison of the observed saturated area and simulated contributing areas by TOPMODEL and HSC
 4 models.

5
 6
 7



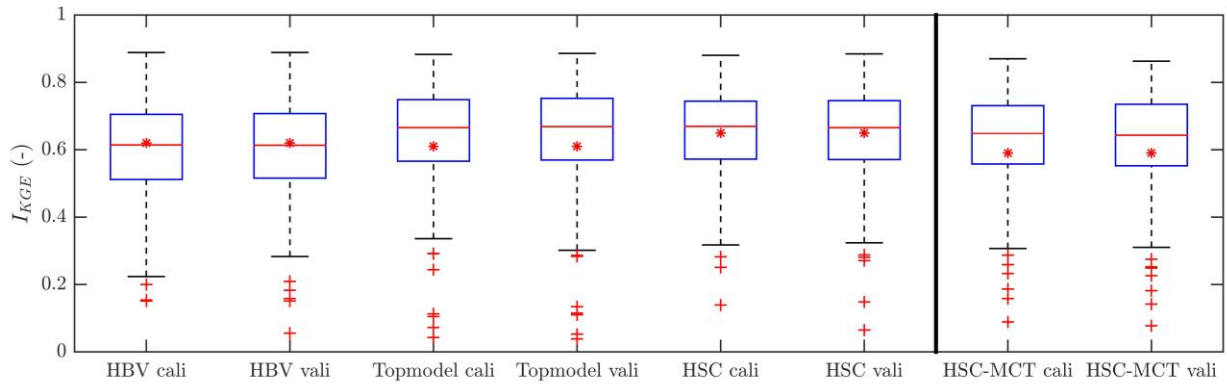
1
2
3
4

Figure 10. The Height Above the Nearest Drainage (HAND) map of the CONUS.



5
6
7
8
9

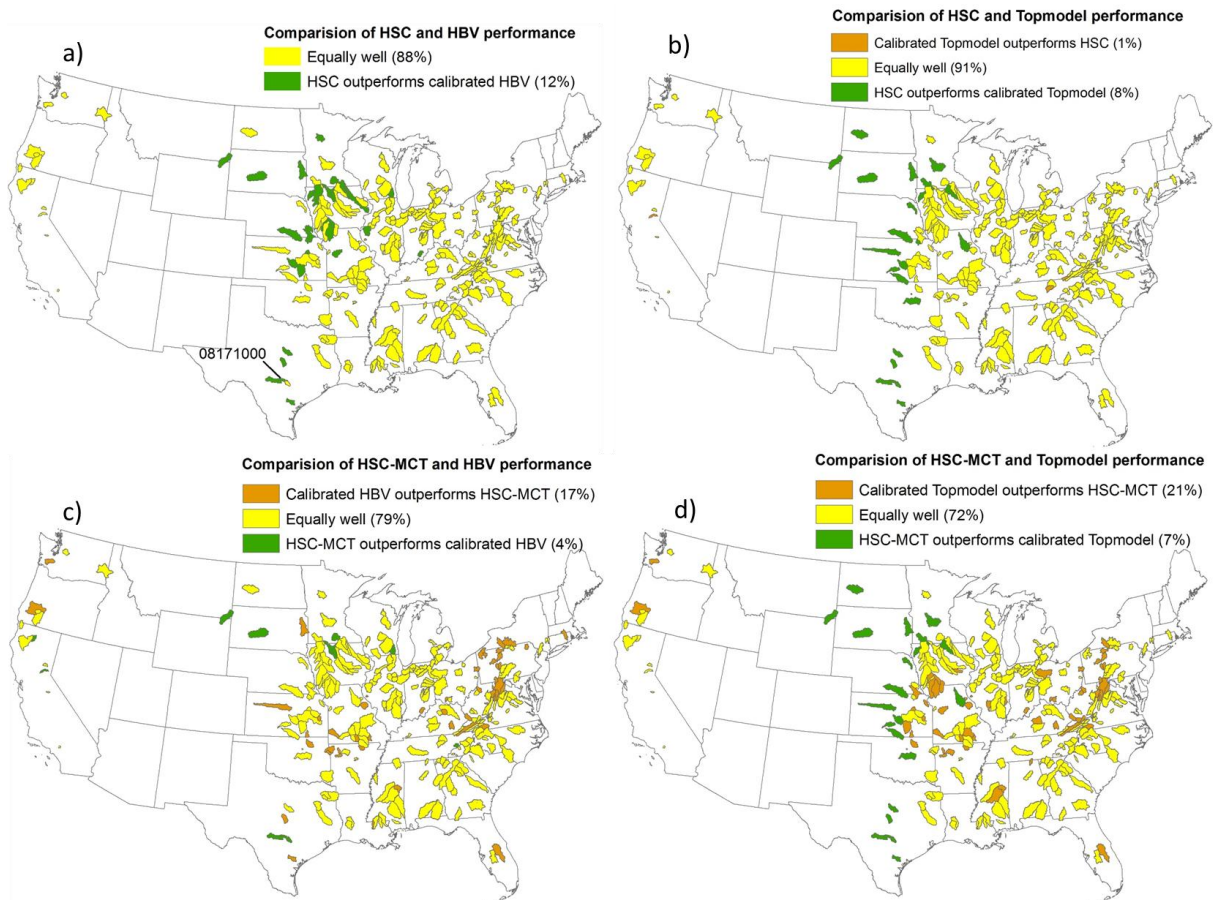
Figure 11. a) The profiles of the normalized HAND of the 323 MOPEX catchments; b) the relations between area fraction and the normalized storage capacity profile of the 323 MOPEX catchments; c) the S_u - A_s curves of the HSC model which can be applied to estimate runoff generation from relative soil moisture for the 323 MOPEX catchment.



1

2 Figure 12. The comparison between the HBV, the TOPMODEL, the HSC, and the HSC-MCT models

3



4

5 Figure 13. Performance comparison of the HSC and HSC-MCT models compared to two benchmarks models: HBV
 6 and TOPMODEL, for the 323 MOPEX catchments.